Portable Solar Desalination System

A Senior Project

Presented to

The Faculty of the Electrical Engineering Department

California Polytechnic State University, San Luis Obispo

In Partial Fulfillment

Of the Requirements for the Degree

Bachelor of Science

By

Genaro Sanchez, Alan Galarza, Erick Del Real

June, 2011

This page intentionally left blank.

TABLE OF CONTENTS

Section *pages*

LIST OF TABLES AND FIGURES

Tables *Page*

Figures

ACKNOWLEDGEMENTS

We would like to thank everyone who has helped us make our senior project possible. First, we would like to thank our adviser Dr. Taufik who gave us the idea for the topic of the project. Dr. Taufik has taken a lot of his time and patience to answer questions, help us look for parts and motivate us to keep looking forward. In addition, we would also like to thank Dr. Prodanov for helping with some of the design ideas although we did not use them. We would like to thank Dr. Dale Dolan as well for helping us interpret the controller's datasheet. Also, the company Ameritherm that took time from their day to lead us in the right direction and for answering emails, phone calls, questions about inductive heating. Finally, we would like to thank the Electrical Engineering Department for allowing us to use the facilities and the equipment needed to work on the project. Thanks again everyone for helping us to make our senior project possible.

ABSTRACT

Clean water and reliable energy can be difficult to obtain in remote locations such as desert villages, secluded islands, and other places where no fresh water can be found. The primary goal for this project is address these problems by implementing a portable desalinization plant system that is to be powered by solar energy PV system as the main energy source.

I. INTRODUCTION

Water is of a great significance for people since it is used for drinking and in food. The human organism must receive a certain amount of water every day. Otherwise, if an organism does not obtain the required amount of water for several days, it dies. It is obvious that the water consumed by the human organism should be pure. Water that contains any harmful bacteria or chemicals may cause various diseases of an organism or even death. Having in mind that 1 % of the world's fresh water is readily accessible for humans. According to the World Health Organization, "Every 15 seconds, a child dies from a water-borne disease 4,500 children die every day because they do not have access to clean drinking water." Each day, in developing countries people have to walk long distances to seek clean water. Often times, this water is contaminated. While we Americans use 80-100 gallons of water daily, people from Africa use about five gallons [1].

Through this project, we explore the possibilities of how to help people in underdeveloped countries to obtain fresh drinking water in a simple, portable, and affordable way. In addition, this project will not only benefit people in the secluded areas but it will also be useful when a natural disaster occurs and the basic services like water are interrupted. The system is to be portable and easy to operate; that is, no complex steps will be required to operate. Hence, just a few of simple steps and the system will do the rest.

II. BACKGROUND

The supply of energy and clean water to remote locations, such as desert facilities, farming operations, resorts, and small villages in the developing world can be logistically complex and expensive. Water is not always easily or readily accessible for many situations. Earthquake stricken countries such as Haiti and Japan suffer the need for clean water. Others have already tried to provide water for those who do not have it. The solution most commonly used is to purchase clean water and then transport it to those who need it. This method can be successful because it delivers ready to drink water. All they need are containers to carry it. The problem with this approach relates to cost that can be expensive. Another solution is to fund sites to drill water wells. When the well is complete, the local village can finally have access to water. The problem with this is that not all well water is clean. Since they are pulling the water from the ground, it may contain contaminants that aren't completely safe to drink. A drawback by using this method is that it doesn't work fast enough when a natural disaster occurs. Drilling a well and installing water purifiers can take up to a year. The price can range from $3000 to $5000 in costs to setup.

One solution that has been proposed is to use green technology to make a portable solar powered desalinization plant. Students and researchers have collaborated at Massachusetts Institute of Technology to create one. This system can clean up 1000 gallons of water per day. It is already portable and ready to be deployed in areas of need. However, this system costs $8000 to construct, and it is fairly large [2]. A system like this isn't quite portable enough to move from location to location assuming there are not methods of transportation on rural areas. In addition, MIT's prototype is easily assembled, but can be

hard to use for people who are not familiar with this technology. Since portability makes the system more convenient, we are proposing a system based on the same concept; providing clean water to people who need it using solar energy while keeping the overall size minimum for portability.

One disadvantage over MIT's prototype is portability. We will stay away from using an adequately large tank to hold water. Our approach is to simply use a moderate size and weight container not larger than 20 gallons to avoid cost and to increase portability. Compared to the MIT prototype, we aren't buying a reverse osmosis pump for our design. Rather we will use a vapor distillation process, which we will construct.

III. REQUIREMENTS

In our design we are going to utilize the energy of the sun to create electric current. The current we obtain is to be inverted to an AC current from its original DC state as shown in Figure 3-1.

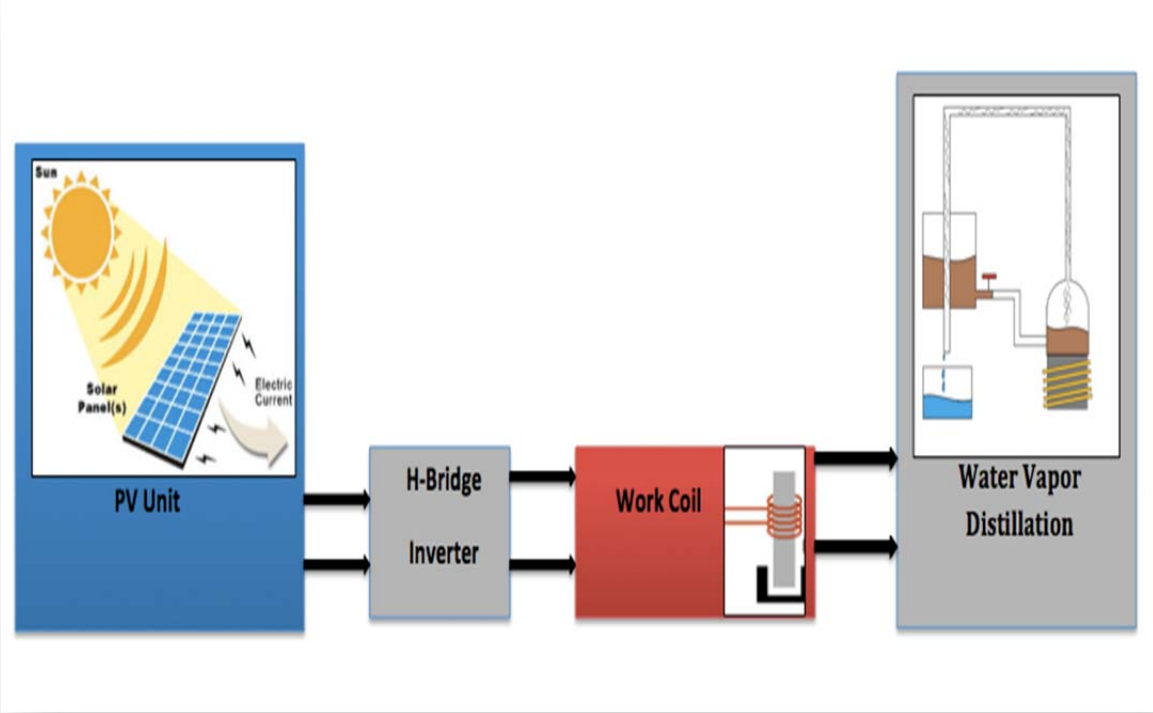

Figure 3-1: Simplified Block Diagram

As shown from the block diagram of Figure 3-1, the system first starts by collecting energy from the sun. The energy received is directly converted to a high frequency ac signal. In turn, this high frequency ac signal is being used to create heat through the coils. This method is known as inductive heating, which is a commonly used technique to generate heat. The heat produced by this inductive heating is then utilized to boil the water in a tank placed in close vicinity of the coil. Eventually, the boiled water changes its physical

state into water vapor, which will then process into vapor distillation from which clean water is acquired.

Electrical Requirements:

The power requirements are sourced from a photovoltaic panel that provides 20 Volts at 5 Amps. The reason for our choice of the PV panel is because it is a clean renewable source. The only thing that it needs is the sun, but the sun is readily available. Secondly, the PV panels do not need any fuel. This reduces costs, and design considerations.

An H bridge topology will be used for the inverter to create the high frequency AC signal. For our coil to generate heat for vapor distillation, we will need a high frequency AC current. We will be designing the H bridge inverter from scratch.

Mechanical Requirements:

In order to minimize heat losses generated by the working coil, we will use an aluminum container due to the fact that aluminum is a very effective heat conductor. In addition, we will enclose the working coil to prevent heat from flowing into the environment and also to minimize losses. The size of the aluminum container is also yet to be determined. We will use a copper coil because it is affordable and it is a relatively good conductor. The volume of water will be targeted to be a few gallons, but its actual size will be determined later as the physical size of the working coil is yet to be decided.

IV. DESIGN

H-Bridge

Inverter

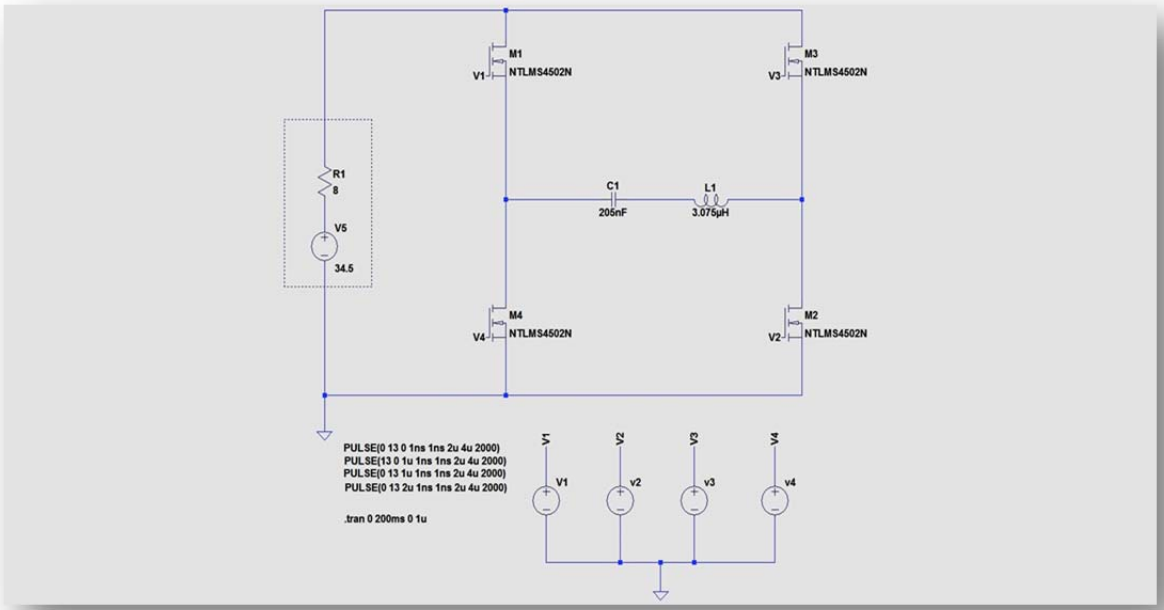

Figure 4-1: Full schematic of the H-Bridge inverter with the thin inductor

An H-Bridge inverter will be able to accept DC power and convert it into AC power for the work coil. The basic schematic of an H-bridge inverter is shown in Figure 4-1. For the full bridge driver we are to use the UBA2035 full bridge driver integrated circuit (IC) that will control the switching of the MOSFETs. The reason why we chose the UBA2035 is because of its ease of use and its ability to drive a full bridge converter with any load.

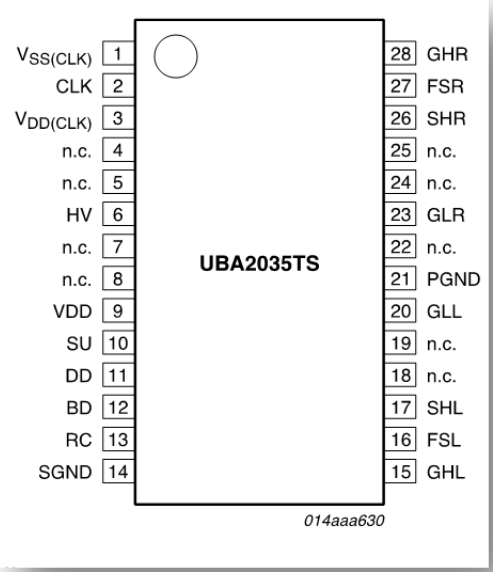

Figure 4-2: UBA2035 IC and its pin outs [4]

In addition, this IC comes as a full bridge controller that makes it suitable for a one chip solution to control the bridge. Also, the UBA2035 is able to generate a frequency of 250 KHz that will increase the heat generated by the work coil. The full bridge controller IC is what establishes the frequency of the switches by manipulating a built in oscillator with a capacitor (C_{osc}) and a resistor (R_{osc}). The manipulation equation is given below [4].

K_{osc} is the oscillator constant and it has a range of .89 (min) to 1.05 (max). R_{osc} and C_{osc} are external components we will use to manipulate the desired frequency on the bridge where the work coil would be located. Hence, by using a standard value of the capacitor of 1 nF and the desired bridge frequency of 250 KHz we can solve for the resistance required. For the oscillator constant we are going to test the controller with both the min K_{osc} and the

max K_{osc} . Keeping this in mind and using the equation provided above, we can solve for the required resistance to achieve a bridge frequency of 250 KHz.

$$f_{BRIDGE} = \frac{1}{K_{osc} * R_{osc} * C_{osc}} \quad (4\text{-}1)$$

$$R_{osc} = \frac{1}{K_{osc} * C_{osc} * f_{BRIDGE}} \quad (4\text{-}2)$$

$$R_{osc} = \frac{1}{0.89 * 1nF * 250KHz} = 4494.38202\ \Omega \quad (4\text{-}3)$$

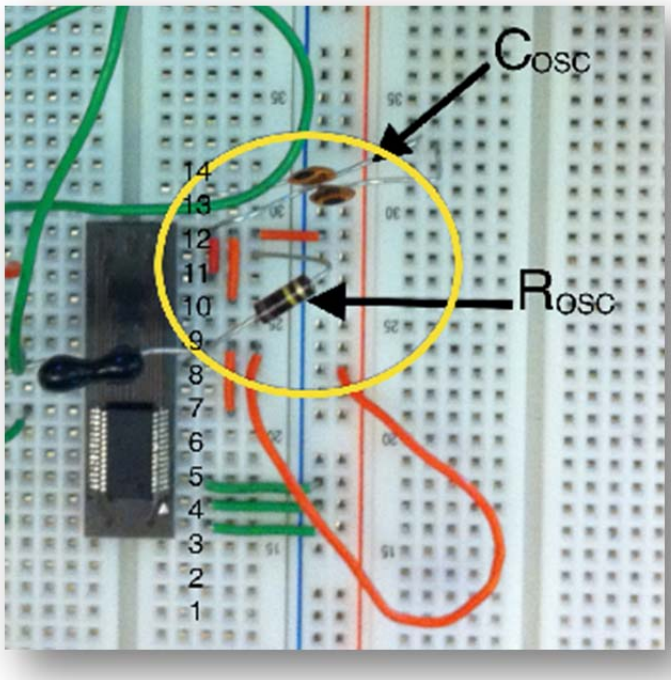

Figure 4-3: R_{OSC} and C_{OSC} connections to the chip

For this calculation we are going to select a standard resistor value of 4.3 K Ω. **Table 4-1** shows the different calculated and standard value resistance.

Table 4-1: UBA2035 Component Specification

Kos	Cosc [nF]	Fbridge [KHz]	Rosc [Ω]	Rosc standard values [KΩ]
0.89	1	250	4494.382022	4.3
0.97			4123.71134	4.3
1.05			3809.52381	3.9

Once the controller is able to generate the desired bridge frequency of 250 KHz, we would then connect it to the H-Bridge to power MOSFETS we selected. The MOSFETS are the actual switches that will be producing the AC output signal to the load (work coil) from the DC input signal. For the MOSFET switches we selected the STPNK60Z because they are fast power MOSFET switches that can handle currents up to 6 A. The PV panel we are utilizing generates a max current of 4.35 A at a max voltage of 34.5 V. The STPNK60Z MOSFETS switches have a max R_{SDON} of 1.2 Ω and can operate safely under 104 W of power dissipation. Following the equation for power dissipation of the switch (MOSFET)

$$P_{MOSFET} = R_{dson} * I_{RMS}^2 * D \quad (4\text{-}4)$$

where R_{dson} is the internal on resistance of the switch, I_{RMS} is the rms current flowing through the switch (from Drain to Source), and D is the duty cycle.

$$P_{MOSFET} = 1.2\Omega * 4.35^2 * 0.5 = 11.3535\ W \quad (4\text{-}5)$$

As shown above the MOSFET switches are suited to endure the power requirements.

In order to deliver maximum power to the load (work coil) we would need to add an impedance matching component to achieve resonance. Since the work coil is inductive (having a positive impedance), a capacitor (negative impedance) would be required to add to the circuit to obtain resonance at 250 KHz. Although we decided to put the capacitor and

the work coil in series, we will test them in parallel to see what gives us the best result. We decided to connect the capacitor and the work coil in series, since based on LTspice simulations the series connections had more current flowing through the coil. Once the circuit operates at resonance, the maximum current will flow through the coil thus giving is a greater change in flux, which means more heat.

Work Coil

Figure 4-4: Thin and thick work coils

In order to obtain maximum flux we decided to add an iron core. The core has a relative permeability of approximately 3000, which makes this a better conductor of flux when compared to an empty core of just air with a permeability of $4\pi E^{-7}$ H/m.

We obtained two pieces of copper wire to create the coils from it as shown in **Figure 4-4**. We decided that we would try out a thick coil and a thin coil with different inductance values to test the H-Bridge circuit and see which one would produce more heat in the core. Once both copper coils were formed, we took the coils to the Power electronics laboratory to measure the inductance in the coils with the iron core. To do this process we were required to use the digital bridge. This tool is used to measure capacitance and inductance at different frequencies, unfortunately the maximum frequency we were able to measure was at 100 KHz. To overcome this problem we were advised by Dr. Taufik to record the inductance and the internal series resistance (ESR) at different frequencies and plot them on an excel graph. Once we recorded and plotted the data we were able to extrapolate the data to approximate and inductance and resistance value for both thin and thick copper coils.

Table 4-2: Thin Coil Inductance and Resistances at Different Frequencies

Frequency [KHz]	L [mH]	R Ω
1	0.0073	1.325
2	0.00647	1.3356
3	0.00604	1.3438
4	0.00576	1.352
5	0.00555	1.3601
6	0.0054	1.3681
6.6667	0.00531	1.3731
7.5	0.00522	1.3794
8.5715	0.00511	1.3877
10	0.00499	1.398
12	0.00485	1.4129
15	0.00468	1.4346
15.385	0.00467	1.4385
16.667	0.00461	1.466
18.182	0.00455	1.458
20	0.00448	1.4724
22.222	0.0044	1.4882
25	0.00432	1.5086
28.572	0.00423	1.5354
33.333	0.00412	1.571
40	0.004	1.6232
50	0.00385	1.7042
66.667	0.00365	1.8486
100	0.00334	2.1672

Table 4-3: Thick Coil Inductance and Resistances at Different Frequencies

Frequency [KHz]	L [mH]	R [Ω]
1	0.00417	0.09932
2	0.00356	0.10699
3	0.00322	0.11409
4	0.003	0.12014
5	0.00282	0.12632
6	0.00269	0.13217
6.6667	0.00261	0.13605
7.5	0.00253	0.14059
8.5715	0.00244	0.14583
10	0.00234	0.1531
12	0.00223	0.16287
15	0.0021	0.17657
15.385	0.00209	0.17812
16.667	0.00205	0.18386
18.182	0.002	0.19052
20	0.00196	0.19662
22.222	0.0019	0.20725
25	0.00184	0.21862
28.572	0.00178	0.23312
33.333	0.00171	0.25204
40	0.00163	0.2779
50	0.00154	0.31648
66.667	0.00143	0.38272
100	0.00128	0.52107

In the tables shown above, we show the inductance and resistances of both the thick and thin work coils at different frequencies. As we can observe, the tool we use to measure the coils could not reach to 250 KHz, therefore we measured the inductances and resistances at all possible frequencies and then plotted them. As shown in **Figure 4-5** through **Figure 4-8**.

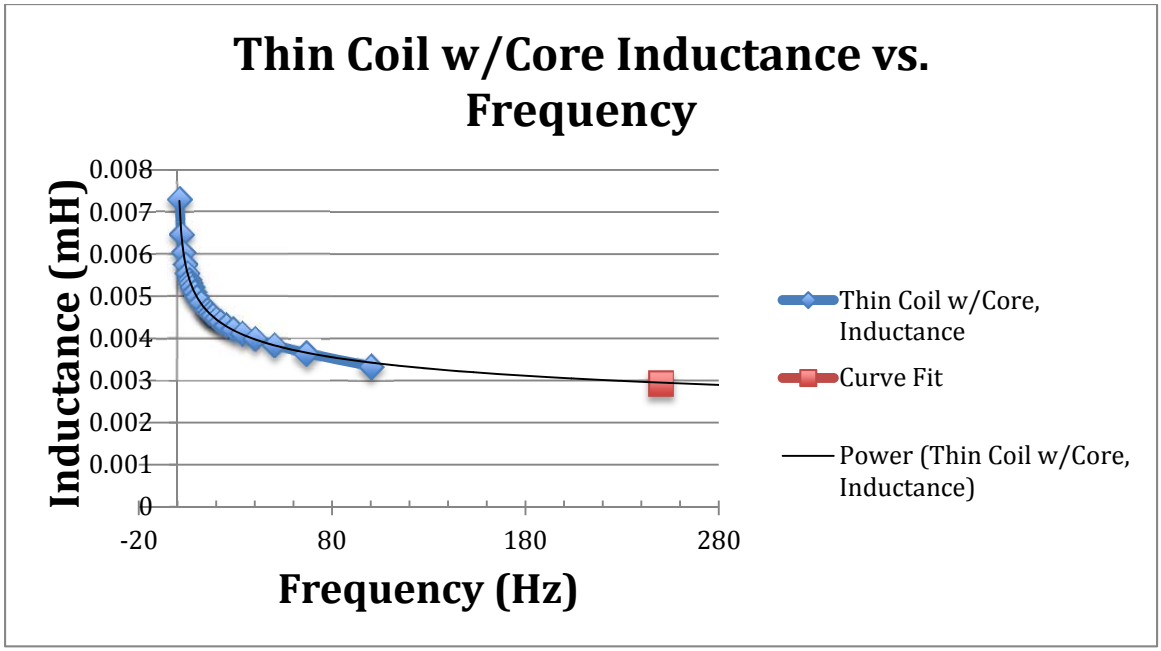

Figure 4-5: Plot of the extrapolated inductance of the thin coil

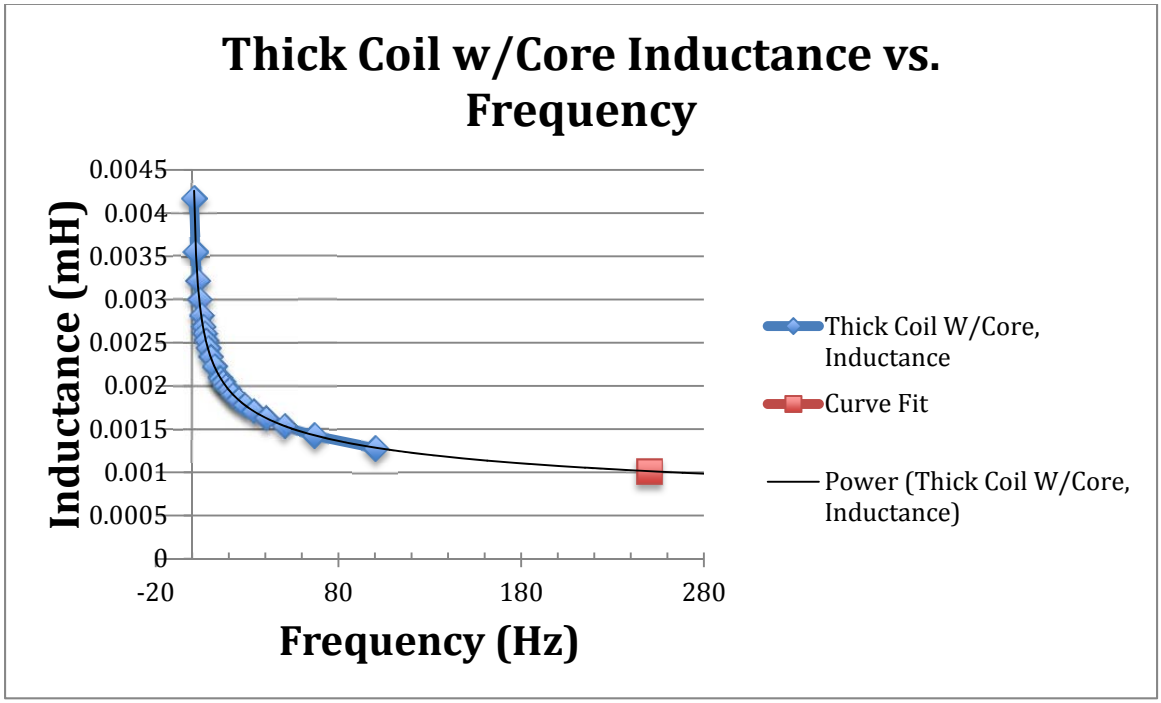

Figure 4-6: Plot of the extrapolated inductance of the thick coil

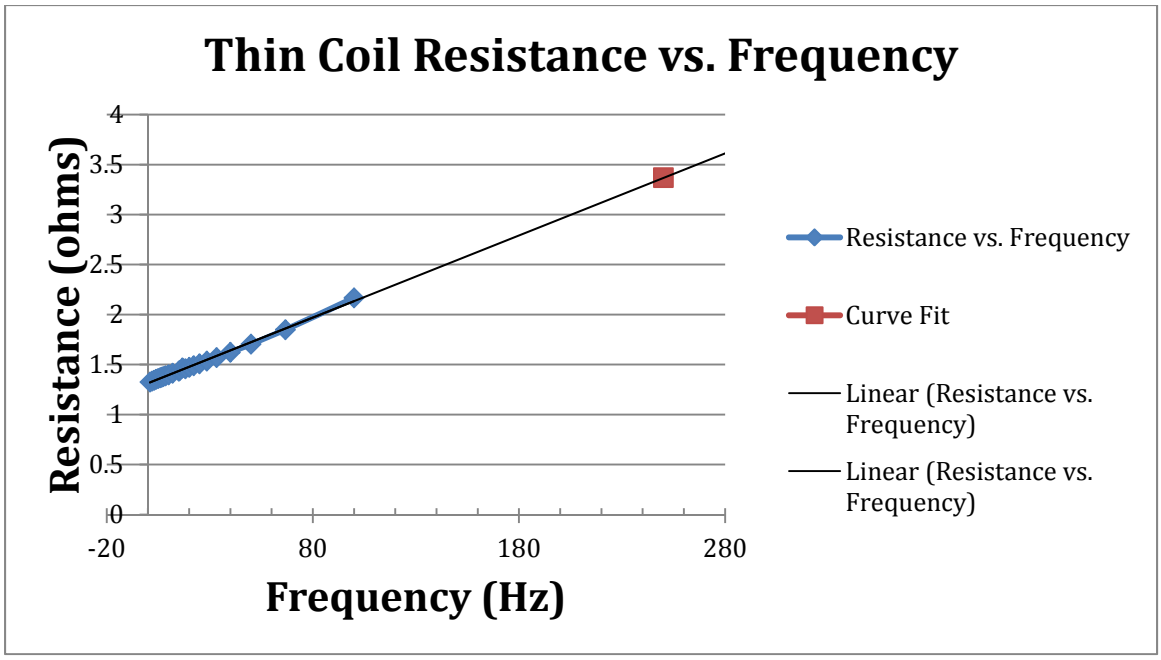

Figure 4-7: Plot of the extrapolated resistance of the thin coil

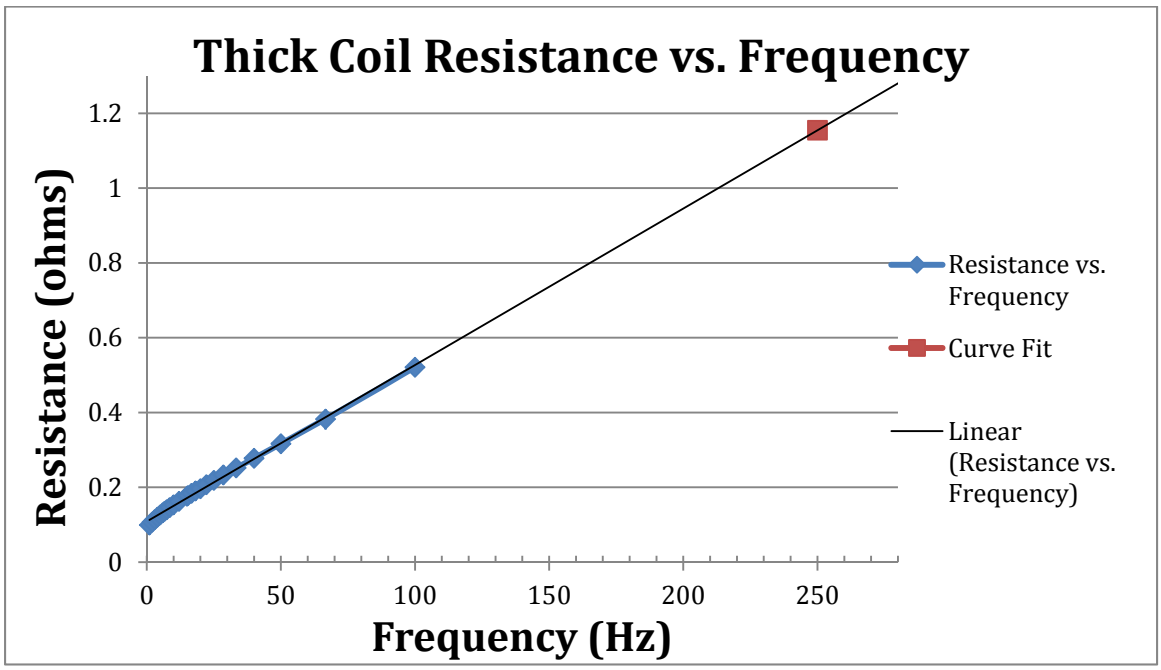

Figure 4-8: Plot of the extrapolated resistance of the thick coil

As shown above, we plotted the inductances of both thin and thick coils, and using Microsoft Excel trend line feature we were able to approximate the expected inductance at 250 KHz. Using the trend lines power regression $Y = 0.0043X^{-0.26}$ and R^2= 0.9996 for the thick inductance coil and $Y = 0.0073X^{-0.163}$ R^2=0.9986 for the thin coil, we approximated L=1.01 μH and L =2.94 μH respectively. The correlation coefficient R^2 denotes the quality of the curve fit. Values for R^2 close to 1 represents a high quality approximation.

The inductance we extrapolated at 250 KHz is as follows:

Thin Inductor L = 2.94 μH

Thick Inductor L= 1.01 μH

The series resistance we obtain by extrapolating the data is as follows:

Thin Inductor R = 3.37 Ω

Thick Inductor R =1.155 Ω

Also we tried measuring the inductance of the thick work coil by applying a $1V_P$ through a series network of a 3.3 Ω and the thick work coil. Using the time constant equation τ = L/R (4-6), and knowing the value of the resistor and τ we calculated L to be as shown in **Figure 4-10**.

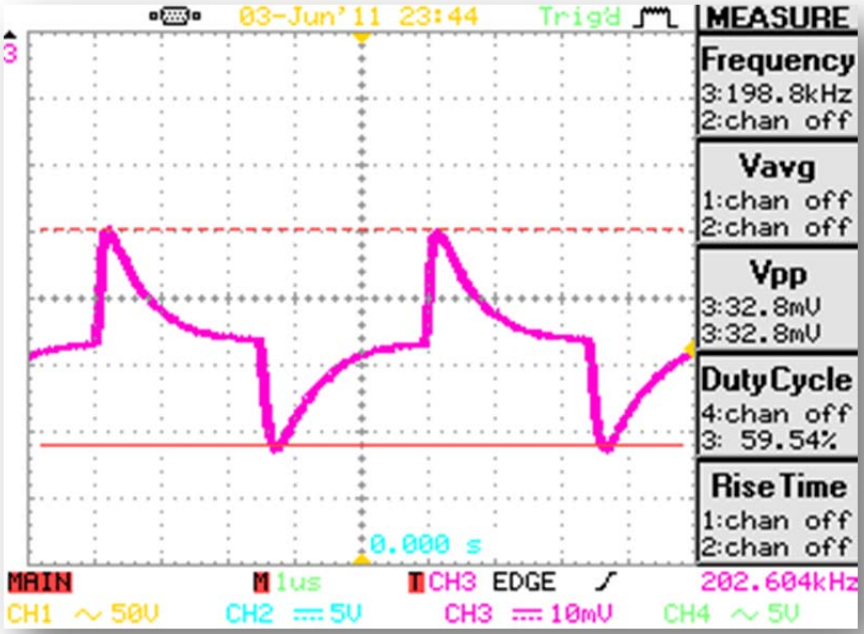

Figure 4-9: Current through the thick coil

$$L_{THICK} = \tau * R = 650ns * 3.5\Omega = 2.275\mu H \quad (4\text{-}7)$$

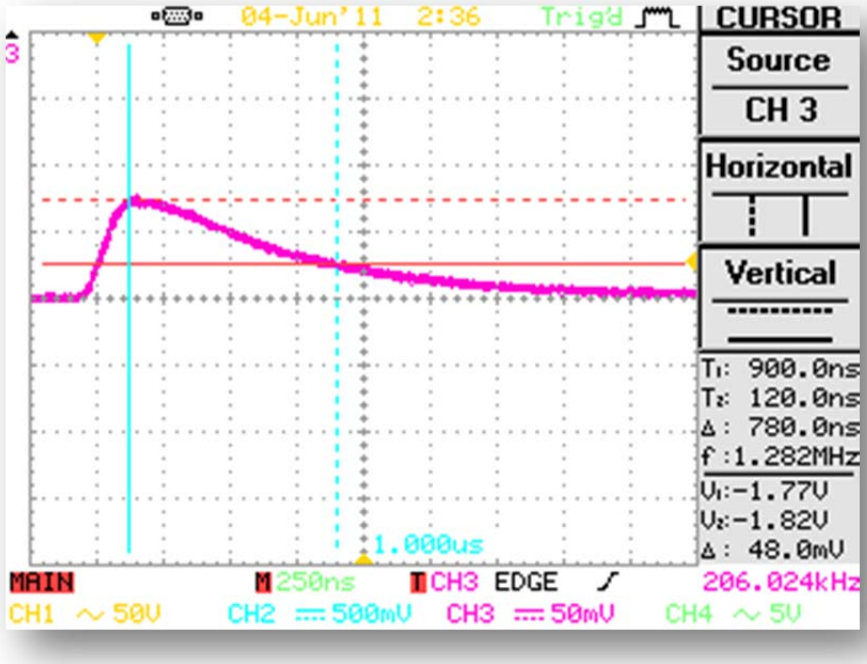

Figure 4-10: Current through the thin coil

The same procedure was repeated for the thin coil to calculate the inductance of the coil.

$$L_{THIN} = \tau * R = 780ns * 3.5\Omega = 2.75\mu H \quad (4\text{-}8)$$

Looking at the data and realizing the resistances for both the thin and thick inductors are big, we consulted with Dr. Taufik to see whether these resistance values were a good idea to use in the simulations. We were advised to measure both coils' resistances with a multimeter, and to use that DC resistance for the simulations.

Once we obtained the work coil inductances and knowing the operational frequency we were able to use the equation below to calculate for the required capacitances.

$$\omega_0 = \frac{1}{\sqrt{L_{THICK\ COIL} * C_{THICK\ COIL}}} \quad (4\text{-}9)$$

$$C_{THICK\ COIL} = \frac{\left(\frac{1}{\omega_0}\right)}{L_{THICK\ COIL}} \quad (4\text{-}10)$$

$$C_{THICK\ COIL} = \frac{\left(\frac{1}{2*\pi*250KHz}\right)}{1.0875\mu H} = 392nF \quad (4\text{-}11)$$

C needed for thick coil = 392 nF

$$\omega_0 = \frac{1}{\sqrt{L_{THIN\ COIL} * C_{THIN\ COIL}}} \quad (4\text{-}12)$$

$$C_{THIN\ COIL} = \frac{\left(\frac{1}{\omega_0}\right)}{L_{THIN\ COIL}} \quad (4\text{-}13)$$

$$C_{THIN\ COIL} = \frac{\left(\frac{1}{2*\pi*250KHz}\right)}{2.94\mu H} = 132nF \quad (4\text{-}14)$$

C needed for thin coil = 132 nF

Once we calculated the capacitance we went ahead and simulated in LTspice to verify the resonance at the desired frequency of 250 KHz.

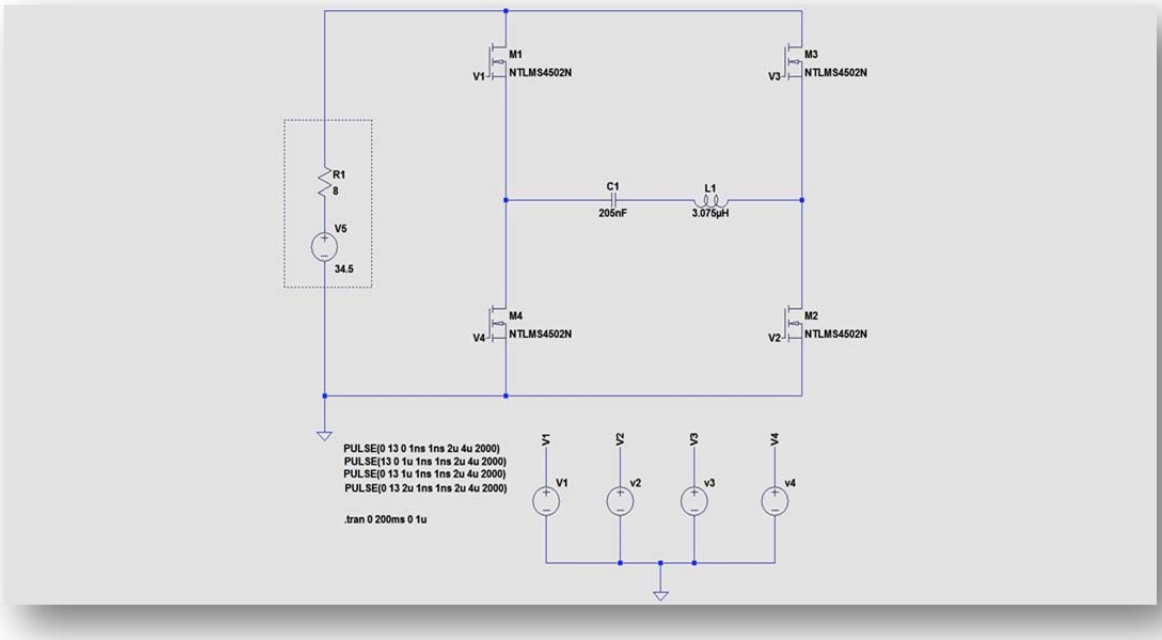

Figure 4-11: Full schematic of the H-Bridge inverter with the thin inductor

In this LTspice simulation, we put the inductance of the thin copper coil and its respective capacitor for resonance.

Figure 4-12 shows a frequency sweep from 10 Hz to 10 MHz of the H-Bridge circuit with the thin coil as a load in series with the capacitor. We can observe that the circuit is at resonance at 250KHz as expected from the calculations.

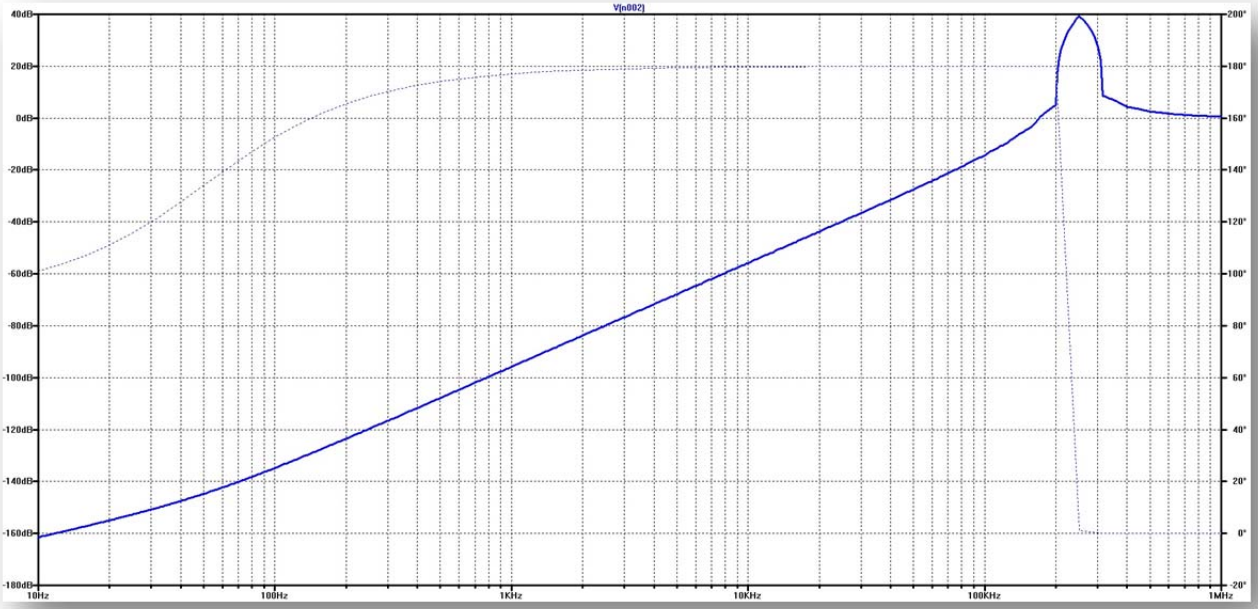

Figure 4-12: Bode plot of the thin coil

Figure 4-13 displays the current seen through the thin work coil. This current is at resonance frequency of 250 KHz. The disturbance seen on the plot is due to the switches having over lap, therefore there is a direct path to ground and no current through the work coil. The UBA2035 controller compensates with dead time between the switches, thus no overlap will occur.

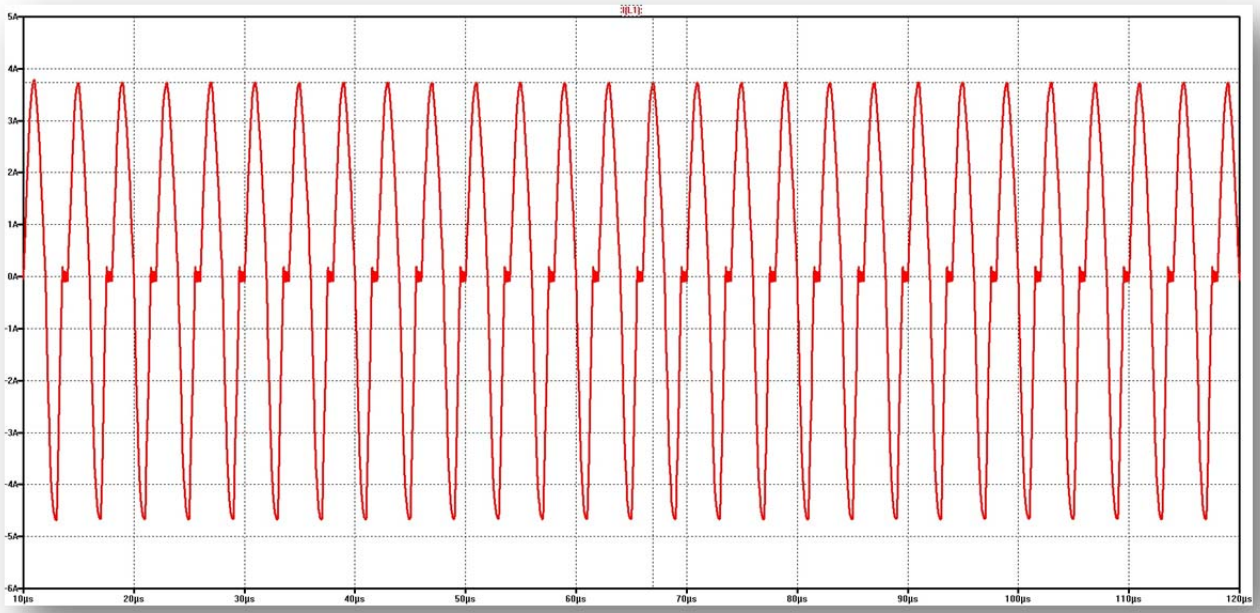

Figure 4-13: LTspice simulation of the current flowing through the thin inductor

In this LTspice simulation, we put the inductance of the thick copper coil and its respective capacitor for resonance. The schematic is depicted in **Figure 4-14**.

Figure 4-14: Full schematic of the H-Bridge inverter with the thick inductor

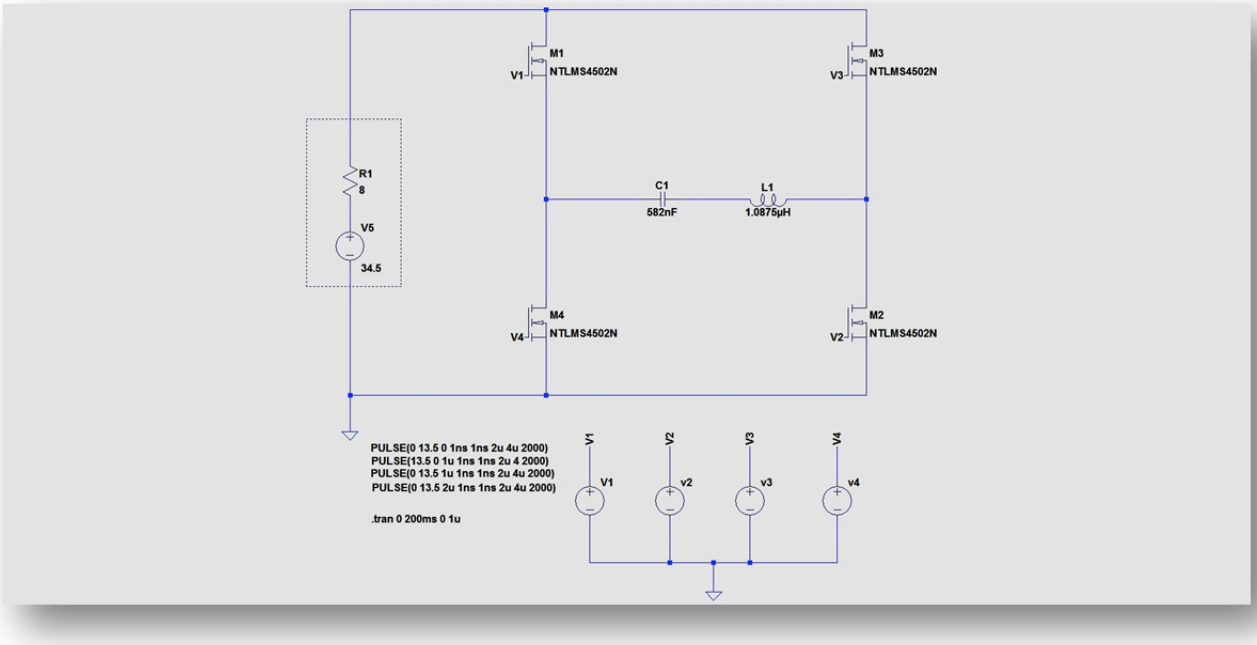

Figure 4-15 shows a frequency sweep from 10 Hz to 10 MHz of the H-Bridge circuit with the thick coil as a load in series with the capacitor. We can observe that the circuit is at resonance at 250KHz as expected for the calculations

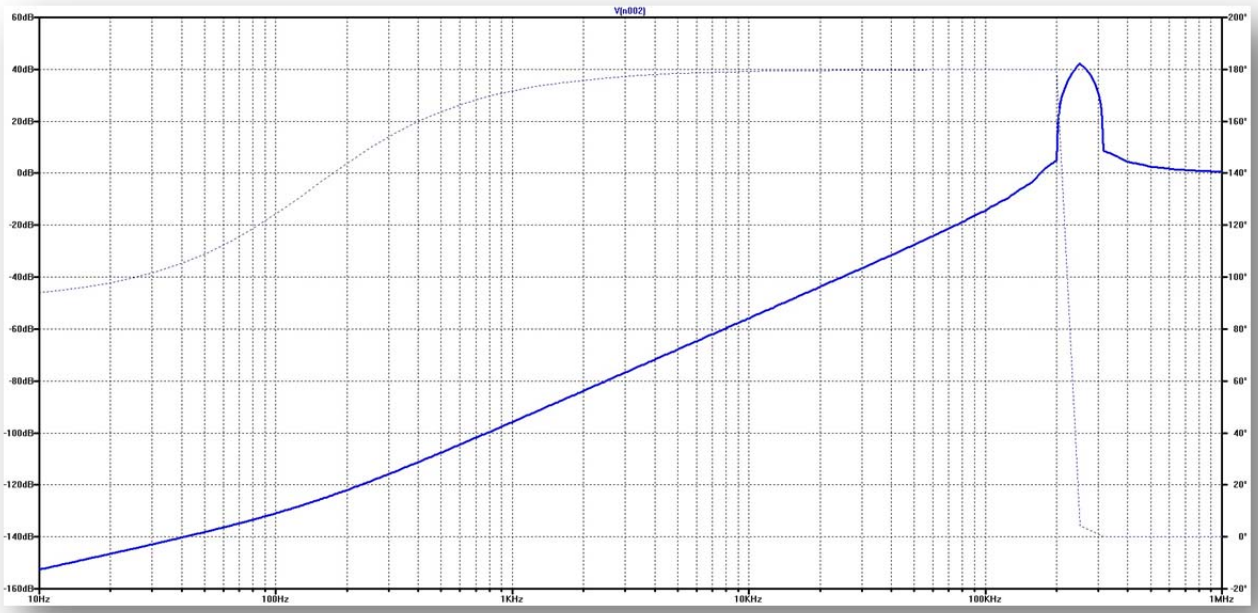

Figure 4-15: Bode plot of the thick coil

Figure 4-16 shows the current seen through the thick work coil. This current is at resonance frequency of 250 KHz. Just as before, disturbance seen on the plot is due to the switches having over lap, therefore there is a direct path to ground and no current through the work coil. The UBA2035 controller compensates with dead time between the switches, thus no overlap will occur.

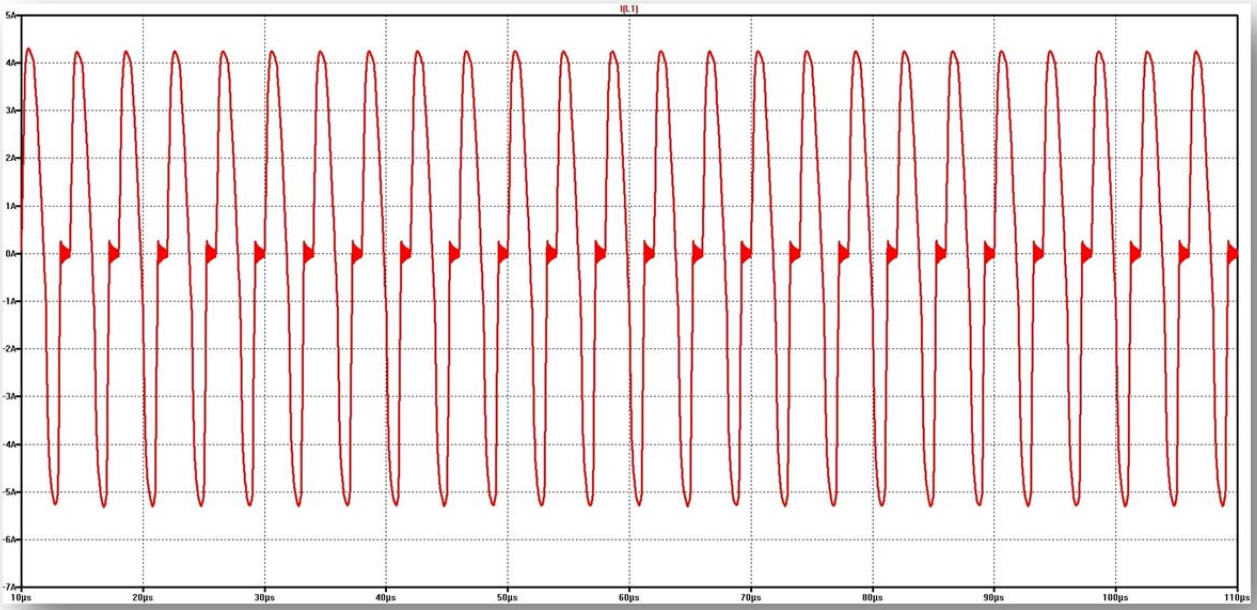

Figure 4-16: LTspice simulation of the current flowing through the thick inductor

The difference of the amplitude of the currents through the thin and thick work coils are due to the different resistances and inductances of the coils. By comparing **Figure 4-13** with **Figure 4-16** we can see that the thick coil is the one that produces greater amplitude in the current. The reason behind it is because there is more copper making it easier for the electrons to flow through it.

Condensation System

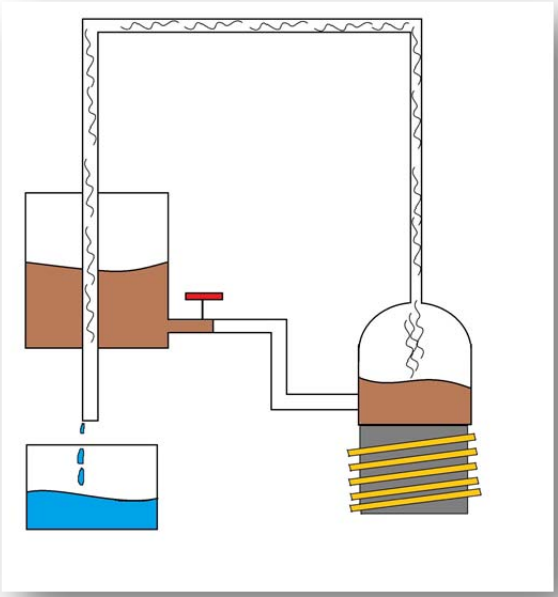

Figure 4-17: Conceptual image of a vapor distillation system.

Using the heat generated from the flux moving through the iron core, we are going to build a vapor distillation system. This method is a very effective way to obtain clean water. Boiling water kills up to 99.99% of all the bacteria that is why it has been used for decades since its simple, efficient, and inexpensive. For third world countries this method will fit perfectly since the necessity of clean water is a priority. By boiling dirty water, any physical contaminants will be left behind in the reservoir. As seen from **Figure 4-17,** there are going to be three main components. The first component is the boiling water container. This component will be used to place dirty water in and is to be placed on top of metal core. The second component is a heat exchanger. A heat exchanger is basically a device that helps transfer heat from one fluid to another without allowing direct contact of the fluids. After doing research into this topic and hearing suggestions from friends whose expertise

is Thermodynamics, we decided to build our own heat exchanger. Regular heat exchangers are very costly; prices can range from $300-1000. This instrument is not highly expensive but also requires a water pump. Therefore, we came to the conclusion of designing and building our own heat exchanger for the purpose of cost and energy efficiency of the overall system. The last but not the least important component is a steam container. Steam container is a large tube capable of holding up to one gallon of steam water.

There will be a small container for the dirty water to rest in. This container will be connected to the boiling reservoir via copper tubing, which is safe for water to travel in. Once the boiling reservoir becomes hot enough, the water will begin to boil. Once the water has become steam, it will travel through more copper tubing. This tubing will be guided back through the dirty water container, which will be considerably cooler. This colder water will condense the hot steam in the pipes into water. At the end of the tubing, clean water will drop out into a third reservoir.

V. CONSTRUCTION AND TESTING

Solar Panels

The solar panel is provided by Dr. Taufik. They are to be used in this experiment once all the other components are working properly. The brand of the solar panel is BP SX 150s has an open circuit voltage of 43.5 V, and a short circuit current of 4.75 A. **Figure 5-1** shows the solar panel used for this project.

Figure 5-1: Image of solar panel to be used for project

In the **Figure 5-2** we can observe the ratings on the solar panel provided by the manufacturer, these ratings are going to be tested to ensure that the data is accurate.

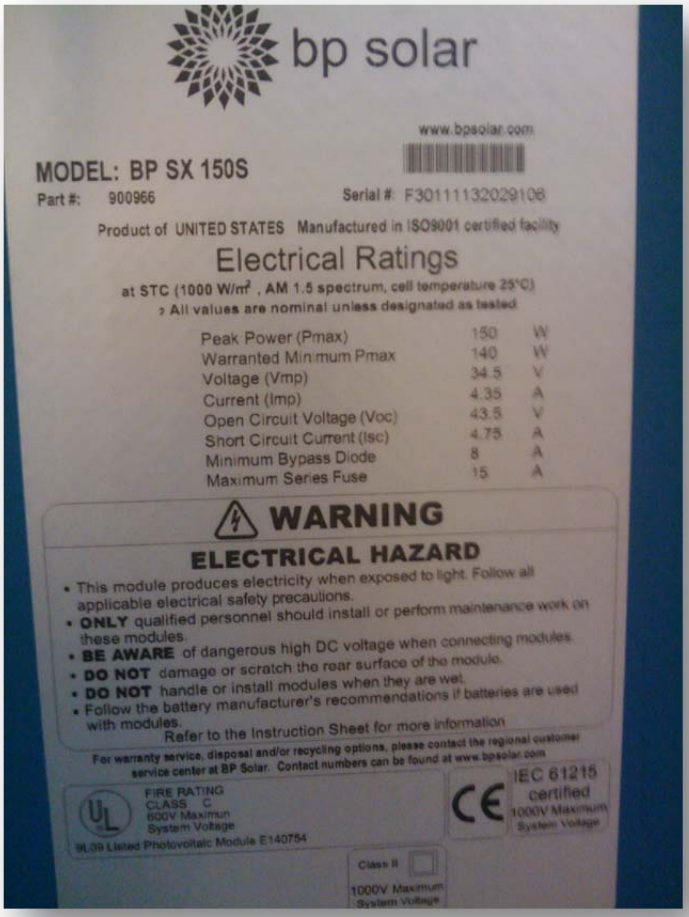

Figure 5-2: Shows the ratings of the BP solar panels.

Two tests that would be critical to perform are the open circuit and short circuit tests with respect to the panel inclination angle. Since the system will be prototyped in San Luis Obispo, the test should then be performed in San Luis Obispo. As it can be observed from **Table 5-1** and **Figures 5-3** and **Figure 5-4**, the panel produces more energy at an

inclination of 24.85 degrees. Since this is this is the location where the panel is to be tested, that would be the angle of horizontal to be used.

Table 5-1: Inclination voltages and currents data

Panel Inclination [degrees]	V_{oc} [V]	I_{sc}[A]
0	37.9	4.65
5	38	4.78
10	38	4.9
15	38.1	4.97
20	38.1	5
25	38.1	5
30	38.1	4.95
35	38.1	4.9
40	38.1	4.8
45	38.1	4.64
50	38.1	4.5
55	38.1	4.29
60	38	4.07
65	37.8	3.86
70	37.7	3.67
75	37.5	3.34
80	37.2	2.96
85	36.9	2.65
90	36.5	2.3

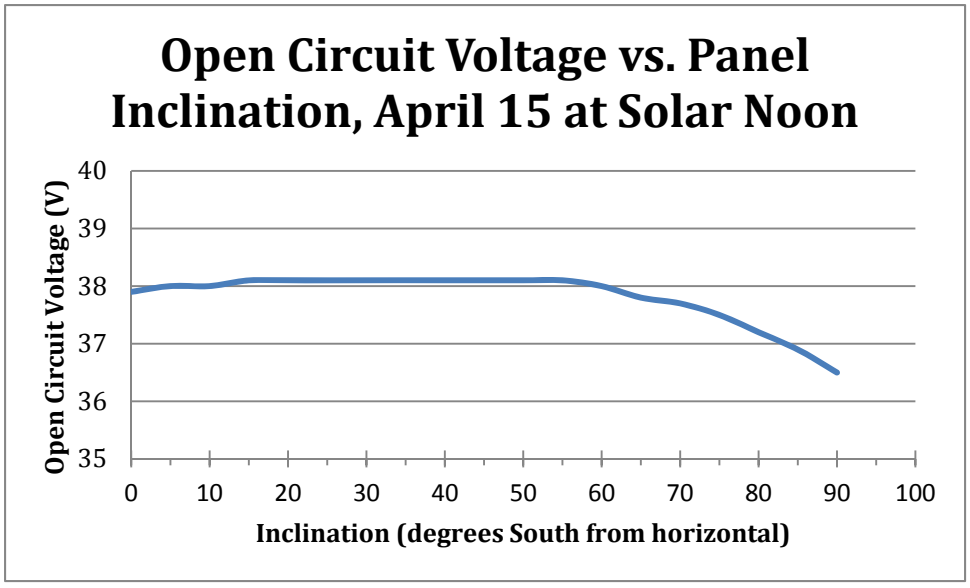

Figure 5-3: Open circuit voltage vs. panel inclination

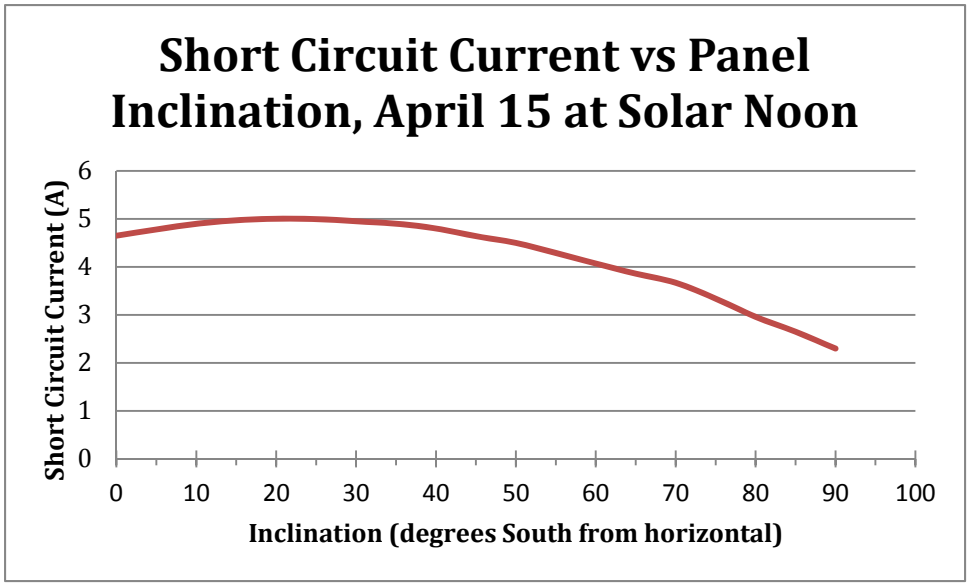

Figure 5-4: Short circuit current vs. panel inclination

The next test that was performed was the I-V characteristics measurement of he panel. The results are shown in **Figure 5-**5, and **Tables 5-**2 and **5-**3. As it was to be expected, the panel would not give us the maximum values as the rated, but through this test we can see more accurate values of what to expect. In addition, we can observe that the maximum power we can obtain using this panel, is when the voltage is at 38.38 V and the current is at 4.50 A that is 172.71 W.

Table 5-2: I-V characteristics data

I [A]	V [V]	R [Ω]	P [W]
0	38.38	#DIV/0!	0
0.2	38.04	190.2	7.608
0.4	37.71	94.275	15.084
0.6	37.37	62.28333	22.422
0.8	37.03	46.2875	29.624
1	36.66	36.66	36.66
1.2	36.28	30.23333	43.536
1.4	35.91	25.65	50.274
1.6	35.55	22.21875	56.88
1.8	35.16	19.53333	63.288
2	34.74	17.37	69.48
2.2	34.32	15.6	75.504
2.4	33.88	14.11667	81.312
2.6	33.4	12.84615	86.84
2.8	32.89	11.74643	92.092
3	32.34	10.78	97.02
3.2	31.67	9.896875	101.344
3.4	30.97	9.108824	105.298
3.6	30.22	8.394444	108.792
3.8	29.34	7.721053	111.492
4	28.15	7.0375	112.6
4.2	26.34	6.271429	110.628
4.4	18.8	4.272727	82.72
4.5	0	0	0

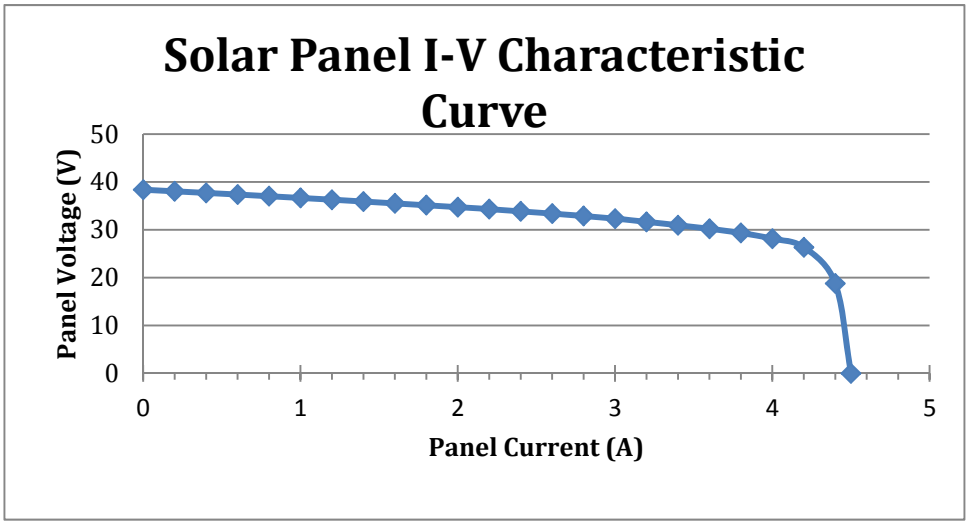

Figure 5-5: Plot of the current vs. the voltage of the panel

Table 5-3: Comparison of the nominal to the measured values

	Voc (V)	Isc (A)	Vmp (V)	Imp (A)	Pmax (W)	Fill Factor
Nominal	43.50	4.75	34.50	4.35	150.08	0.73
Measured	38.38	4.50	28.15	4.00	112.60	0.65

H-Bridge (no load)

Figure 5-6 shows that there are 5 key components of the H-bridge inverter: the UBA2035T Full bridge controller, and the 4 STP6NK60Z MOSFETS. To eliminate noise, we soldered the H-bridge to a protoboard. This protoboard is capable of withstanding a higher level of amperage than a breadboard. We had burnt four UBA2035s throughout the entire testing process. All four, which were burnt, had load attached to them. We decided to monitor the gate signals and output voltages before loading the H-bridge. This allowed us to determine if the right signals were being sent at the correct frequencies.

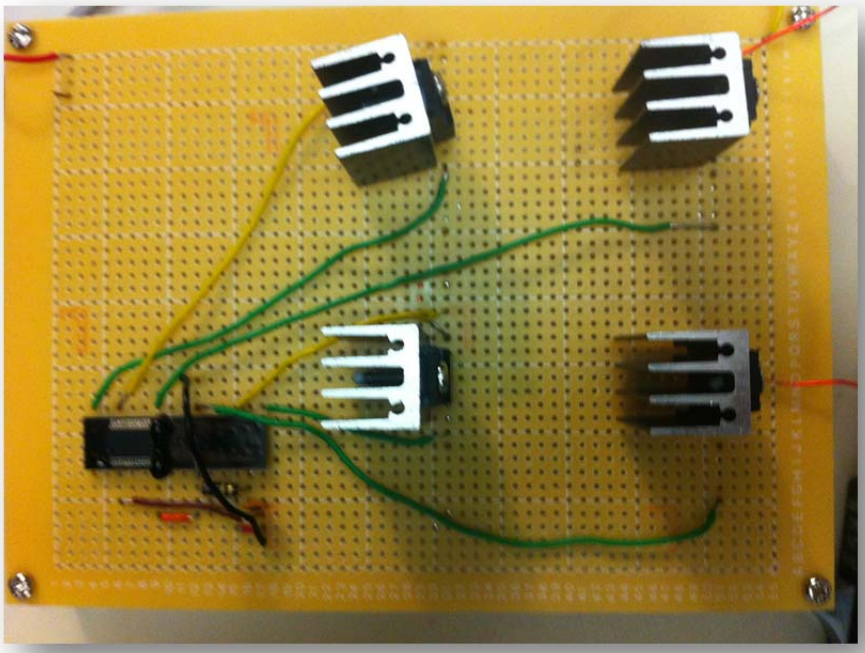

Figure 5-6: Image of the H-bridge inverter

Throughout this process, we had to recalculate some of the values, which were calculated earlier in the design. First of all, we concluded that it would be best to remain at a frequency of 200 KHz. We chose to do this because the highest possibly frequency allowed by the controller is 250 KHz. This is only possible when we get the right oscillation constant K_{osc}, which is not a variable we can control. The value of K_{osc} is a parameter that is controlled by the quality of the chip, and the testing parameters for the UBA2035. As listed, K_{osc} ranges from 0.89 to 1.05 with 0.97 being the typical value [4]. However, this value was obtained for an oscillation frequency of 500 Hz. When we had calculated an oscillation frequency of 250 KHz and used new values for R_{osc} and C_{osc} as 150KΩ and 32pF, respectively. Yet the oscillation frequency we measured was 108 KHz. So now using equation (4-1) with the new R_{osc} as 100 KΩ, C_{osc} as 10pF and F_{bridge} set to 200 KHz, we calculated K_{osc} to be 5Using these new values, we were able to obtain gate signals which oscillated at approximately 200 KHz. All UBA2035s we used were sourced by a 12.5 V_{DC} and a limited current of 200 mA.

Both gate signals seen in **Figure 5-2** and **Figure 5-8** are for the upper-left and upper-right MOSFETS in the H-bridge. Each signal has a DC-offset of 7.4 V_{DC}, and oscillates between 11.5 and 7.4 V_{DC} at a frequency of 196.24 KHz. The UBA2035 sends 4 voltage signals for the MOSFETS: 2 gate signals, and 2 source voltages. The source voltages set the upper MOSFETs sources to a higher potential than ground. When the gate signal goes high, the difference in potential between the source and the gate allow the MOSFET to conduct. When the gate signal goes low and matches the value seen on the source, the MOSFET's channel closes and cannot conduct current.

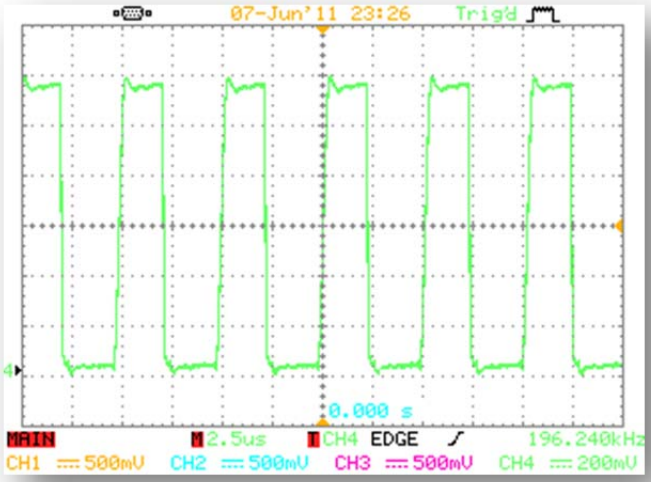

Figure 5-7: Unloaded UBA2035 output signal pin 15 (V_{GHL})

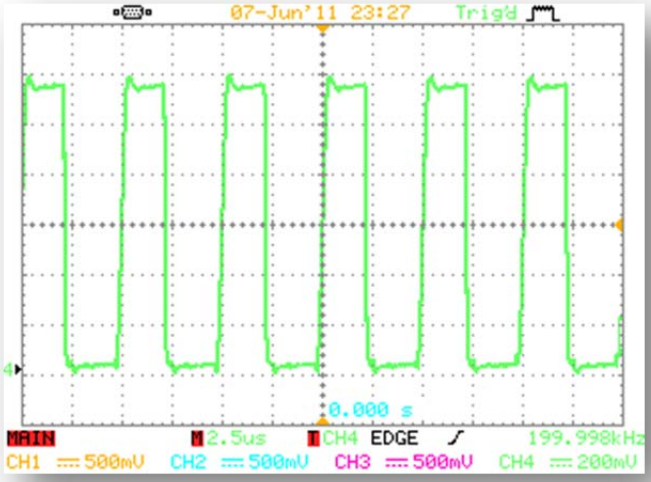

Figure 5-8: Unloaded UBA2035 output signal pin 28 (V_{GHR})

The two images shown in **Figure 5-9** and **Figure 5-10** are the output signals for the two lower MOSFETS. These signals oscillate from 0 to 12.5 V_{DC} at a frequency of 198.614 KHz. Unlike the upper MOSFETs, the sources on these switches were tied to ground (PGND, pin 21).

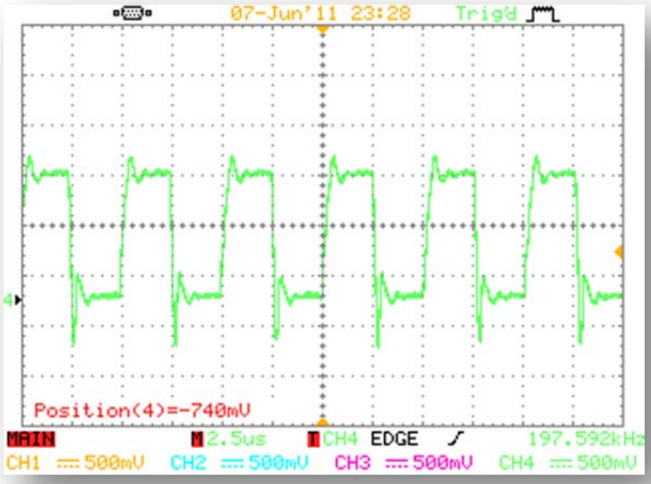

Figure 5-9: Unloaded UBA2035 output signal pin 20 (V_{GLL})

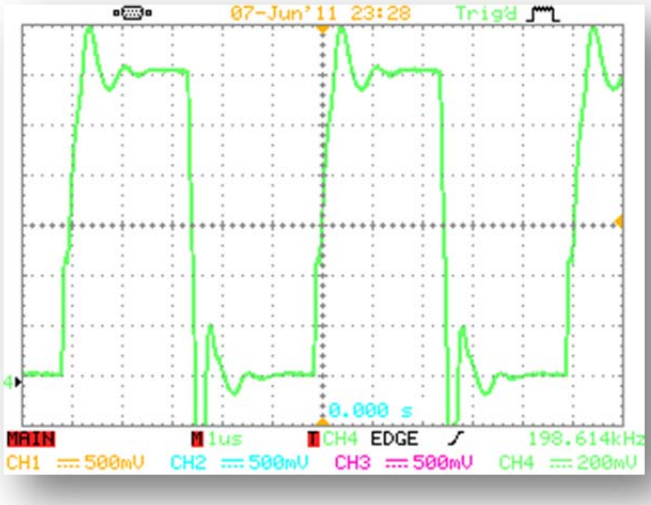

Figure 5-10: Unloaded UBA2035 output signal pin 23 (V_{GLR})

H-Bridge (loaded)

Once we had observed the output signals of our unloaded UBA2035 chip, we decided to attach three different resistive loads to observe and analyze our H-bridge inverter's performance. But even after simply connecting the H-bridge to the controller, it did not behave as expected (at first). The upper two MOSFET's gate signals were denatured after even light loading while the two bottom gate signals remain unchanged.

To measure current, we used the current probe. When the oscilloscope is marked at 10mV/division that directly translates to A/division based on the current probe's knob. When the oscilloscope does not display 10mA/division, the equation to calculate the A/division is

$$\frac{Oscilloscope\ (mV/Division)}{10mV/Division}\ x\ (Current\ value\ on\ the\ knob) \qquad (5\text{-}1)$$

Load One: 1000Ω

Figures 5-11 through **Figure 5-14** are the gate output signals driven by the UBA2035. The UBA2035 emits 8 signals in its entirety. Four of the signals sent (V_{GHL}, V_{GHR}, $V_{GLL,}$ V_{GLR}) are 200 KHz signals sent to the gates of the MOSFETS to control the switching. Two DC signals (V_{SHL} and V_{SHR}) are sent to the upper MOSFETs' sources. The last two signals (V_{FSL} and V_{FSR}) are the upper voltage rails for oscillation as explained later. **Table 5-4** shows the expected voltages for oscillation based upon the UBA2035 datasheet [4]. The upper signals are expected to oscillate between V_{FSR} and V_{SHR}. The values of V_{FSR} and V_{SHR} are expected to be equal to V_{FSL} and V_{SHL}. The signals shown in **Figure 5-11** and **Figure 5-12** are the gate signals for the upper left and right MOSFETs, respectively. With proper operation, both are supposed to oscillate from 11.68 to 3.45 V_{DC} with a DC offset of 3.45 V_{DC}. But once they are loaded with 1000 Ω, they do not show the DC offset that is expected. They still switch, but they drop below 3.45 V_{DC}. At the same time, they do not look as "clean" as those signals seen in **Figure 5-7** and **Figure 5-8** in the unloaded cases. The signals seen in **Figure 5-13** and **Figure 5-14** do oscillate from their expected values of 12.5 (V_{DD}) to 0 (ground). Again, the only discernable difference is that the signals are not as "clean" as the unloaded gate signals seen in **Figure 5-7** and **5-8**

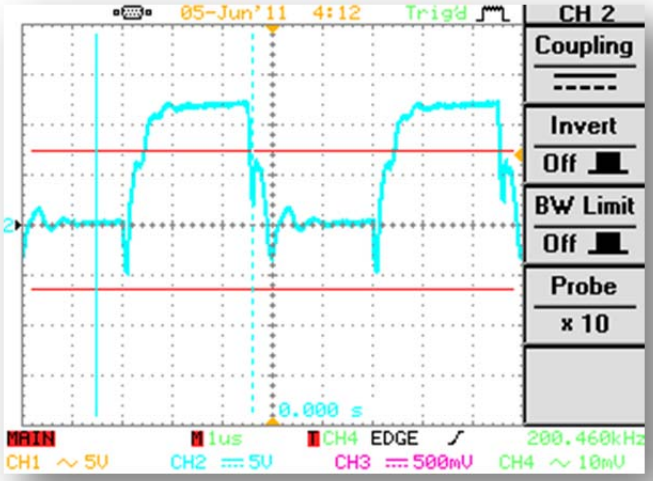

Figure 5-11: Loaded UBA2035 output signal pin 15 (V_{GHL})

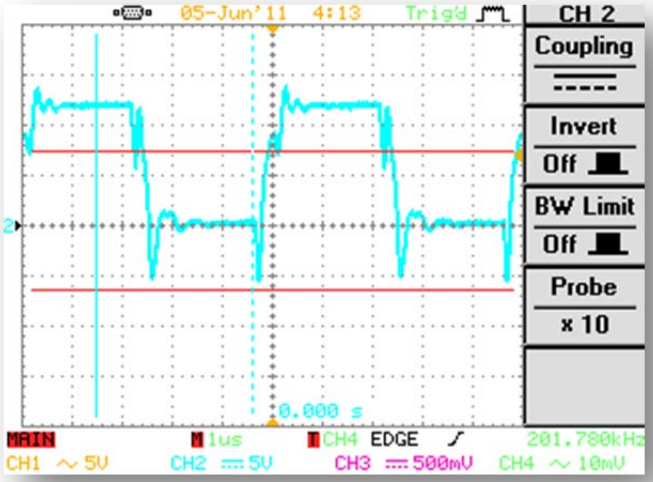

Figure 5-12: Loaded UBA2035 output signal pin 28 (V_{GHR})

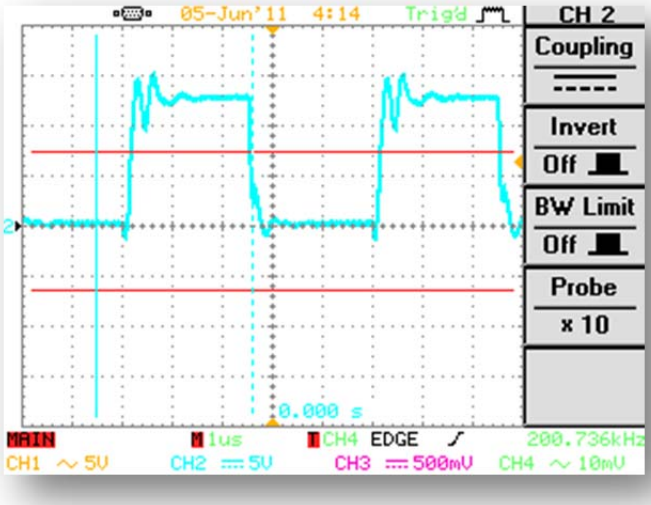

Figure 5-13: Loaded UBA2035 output signal pin 20 (V_{GLL})

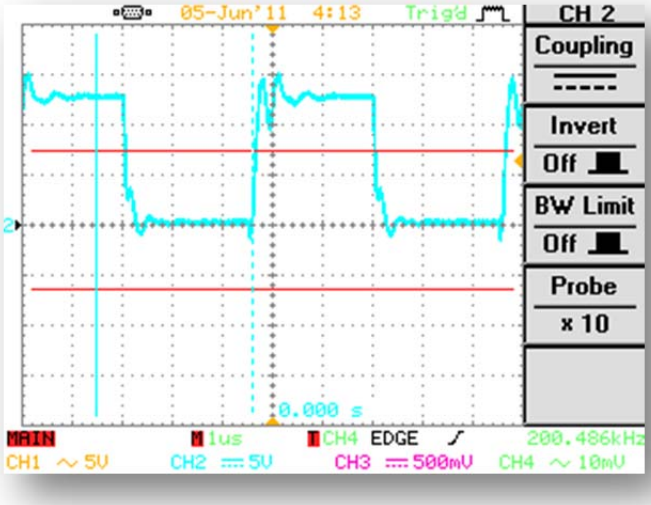

Figure 5-14: Loaded UBA2035 output signal pin 23 (V_{GLR})

Table 5-4: UBA2035 Output Voltages

UBA2035 Pin no.	Signal Name	V_{DC}
27	V_{FSR}	11.68
26	V_{SHR}	3.45
16	V_{FSL}	11.68
17	V_{SHL}	3.45

Comparing these values to the datasheet, we concluded that these values were within expected parameters.

As shown in **Figure 5-15** the scale is 10mV/division for the current across the 1000Ω. As configured on the current probe, each 10mV/division seen on the oscilloscope corresponds to 1mA/division. This means the peak-to-peak value of this current is 7 mA.

After allowing one minute for the circuit to operate, the chip started to break down. The top two MOSFETs switching frequency spiked up while the amplitude went low. The lower two MOSFETs appeared to be working as expected.

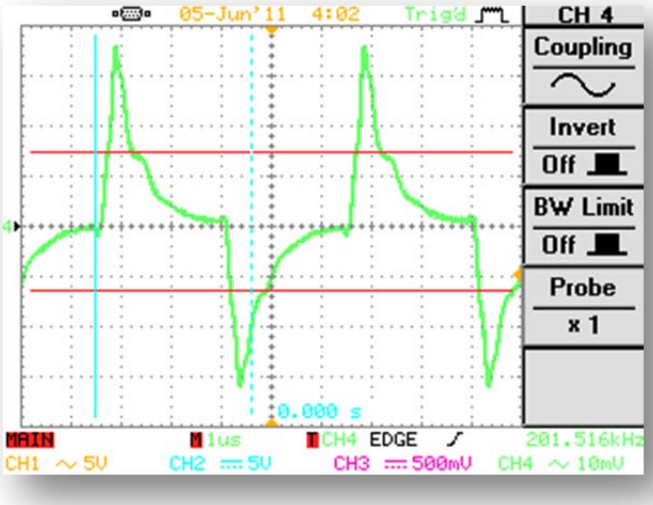

Figure 5-15: Current across 1000Ω load

Load Two: 120Ω

As was the case for the 1000Ω load we attached to the H-bridge inverter, the lower two gate signals viewed in **Figure 5-18** and **Figure 5-19** oscillated from the expected values of 12.5 to 0 V_{DC}. The upper two MOSFETs showed no DC offset as expected although they did oscillate within expected parameters as explained on Page 46.

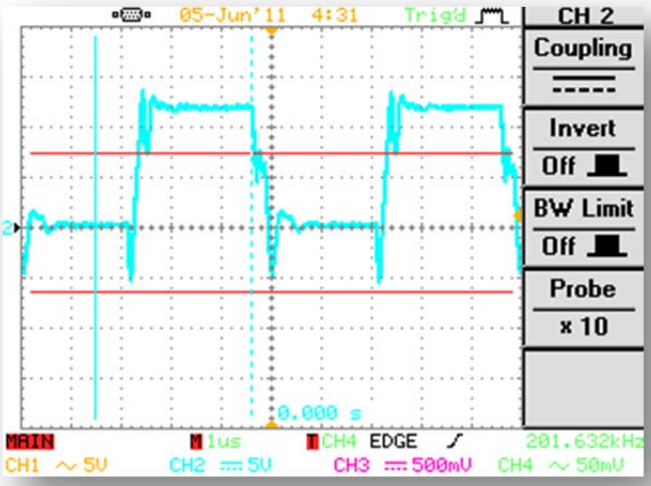

Figure 5-16: Loaded UBA2035 output signal pin 15 (V_{GHL})

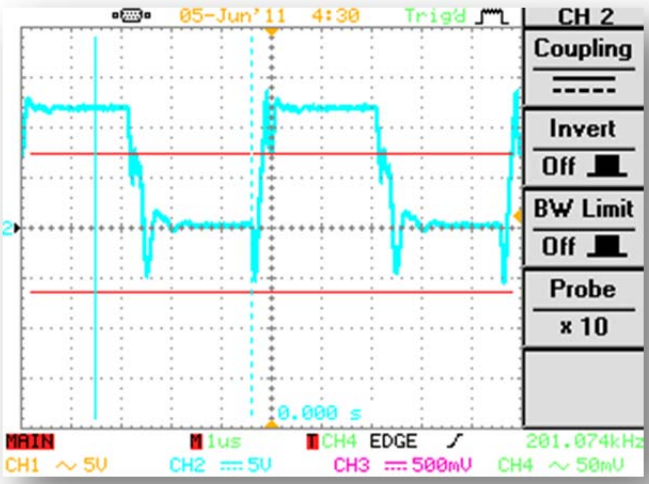

Figure 5-17: Loaded UBA2035 output signal pin 28 (V_{GHR})

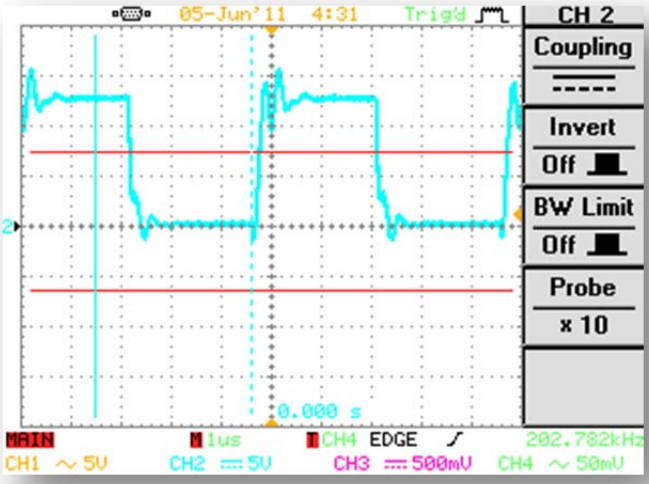

Figure 5-18: Loaded UBA2035 output signal pin 20 (V_{GLL})

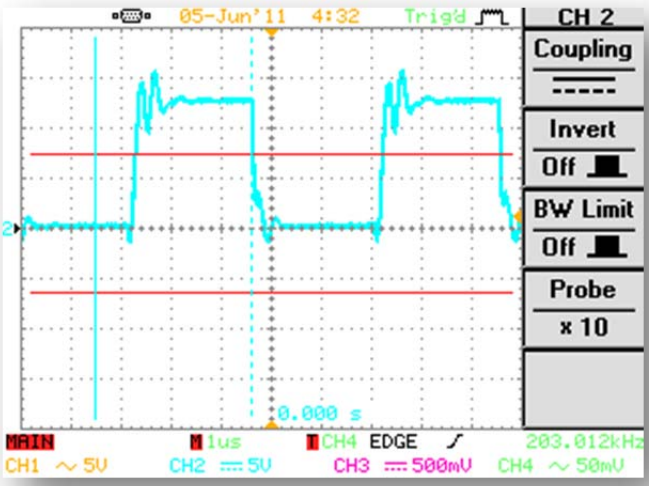

Figure 5-19: Loaded UBA2035 output signal pin 23 (V_{GLR})

Table 5-5: UBA2035 Output Voltages

UBA2035 Pin no.	Signal Name	V_{DC}
27	V_{FSR}	11.59
26	V_{SHR}	3.27
16	V_{FSL}	11.59
17	V_{SHL}	3.27

As shown in **Figure 5-20** the scale is 50mV/division. The value of the knob on the current probe was 1mA/division. Using equation (5-1), we can calculate the A/division for the current probe, which calculates to 5mA/division. This number translates to a 22 mA_{PP} current through the 120Ω load.

$$\frac{50mV/division}{10mV/division}\ x\ \left(\frac{1mA}{division}\right) = 5mA/division \qquad (5\text{-}2)$$

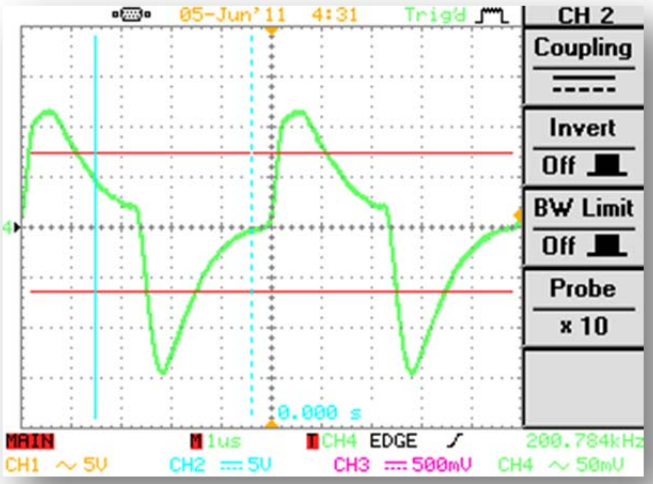

Figure 5-20: Current across 120Ω load.

Load Three: 10.2Ω

The gate signals seen for the upper MOSFETs gate for this load in **Figure 5-21** and **Figure 5-22** were very distorted compared to expected values. Rather than oscillating from above 11 V_{DC} to approximately 3 V_{DC}, they both only reached maximum amplitude of 600 mA. They also did not show the expected DC offset as was seen in the unloaded case. The only signal that oscillated near 200 KHz was the upper left MOSFET as observed in **Figure 5-21**. The other three signals seen in **Figure 5-22** through **Figure 2-24** oscillated at 190 KHz, 390 KHz, and 393 KHz respectively. The lower two MOSFET gate signals seen in **Figure 5-23** and **Figure 5-24** did oscillate from 12.5 to 0 V_{DC} as expected.

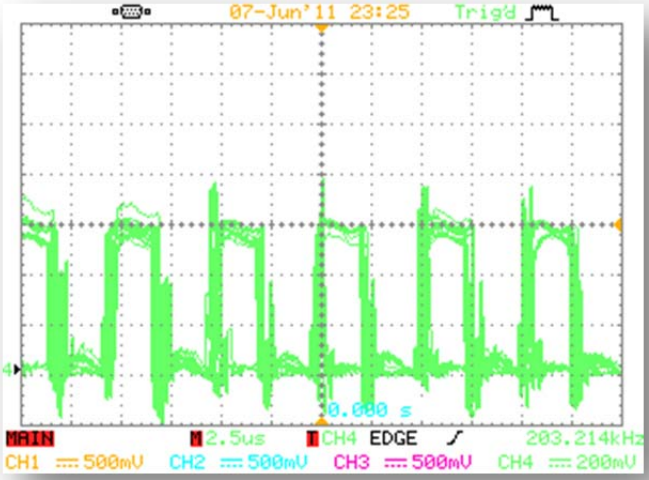

Figure 5-21: Loaded UBA2035 output signal pin 15 (V_{GHL})

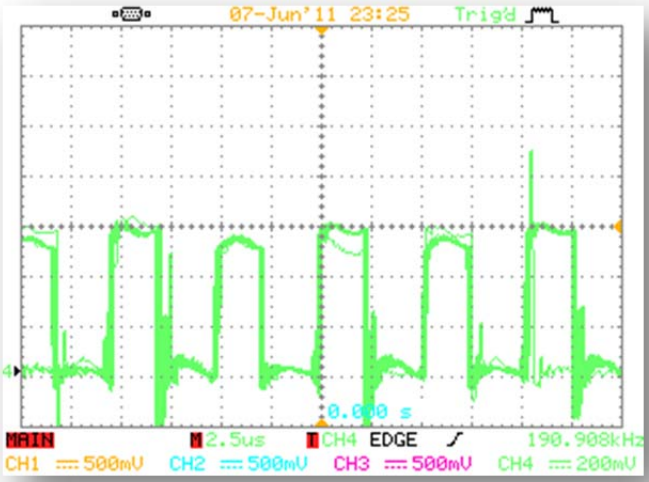

Figure 5-22: Loaded UBA2035 output signal pin 28 (V_{GHR})

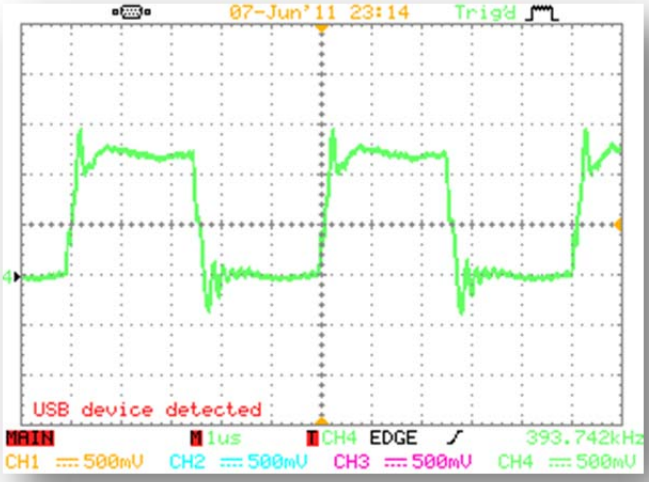

Figure 5-23: Loaded UBA2035 output signal pin 20 (V_{GLL})

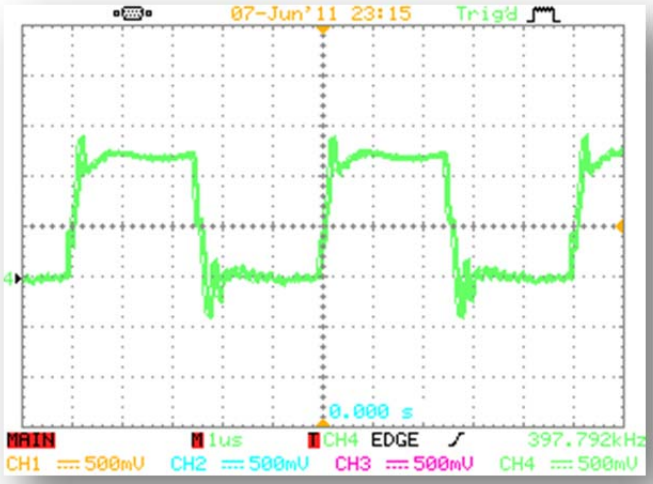

Figure 5-24: Loaded UBA2035 output signal pin 23 (V_{GLR})

Table 5-6: UBA2035 Output Voltages

UBA2035 Pin no.	Signal Name	V_{DC}
27	V_{FSR}	10.51
26	V_{SHR}	2.07
16	V_{FSL}	10.51
17	V_{SHL}	2.07

As seen in **Figure 5-25**, we no longer had a full AC signal on the load. It also did not oscillate at our designed value of 200 KHz but rather 186 KHz. The gate signals all worsened with this load. Soon thereafter, this chip burnt out as well.

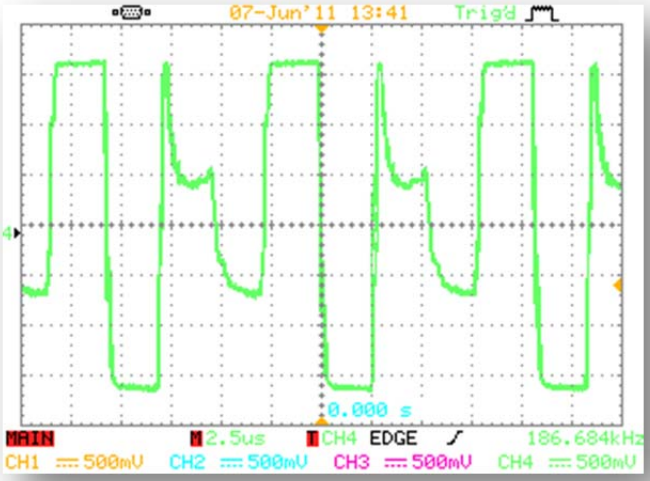

Figure 5-25: Current across 10.2Ω load

Figure 5-26: 10.2Ω resistive load. Capable of dissipating 500W.

Work Coils

Our original design called for our work coil load to be in series with capacitors. However, after further consideration we decided to place the capacitor bank in parallel with the work coil. This achieves a higher current through the coil and less stress on the capacitors in terms of heat dissipation.

Throughout the duration of testing, the thick work coil broke. As we tried to approximate the value of the inductance of the thick coil, we unfortunately wore down the epoxy we used to maintain the coil at a fixed position. By introducing the core into the thick coil, removing it from the coil, and taking it to different benches to use the different equipment, the epoxy that maintained the coil in fixed position broke. After this, the coil was no longer stable and had movement like a spring. This movement directly affects the inductance of the thick coil and made it unreliable for further testing. If the H-bridge were to be built using the coil whose inductance was not stable, it would be difficult to achieve resonance in the bridge. Since the thin coil is wider the core can be inserted without any risk of damaging the coil. This makes the thin coil more reliable.

The one concept that still remained was for our load to remain at resonance for a 200 KHz signal. With our load at resonance, less strain would be placed upon the UBA2035. The load would be considered an ‘open’ and would require less gate current drawn through the MOSFETS from the UBA2035. The resistive loads that we had tried earlier were demanding more current from the IC and breaking our chips. With a high frequency of 200 KHz, it is very important to have our load achieve resonance or else it will also break the ICs with its demand of gate current.

For our load, a capacitive bank was used in parallel with the inductive work coil and core to achieve resonance. One nuance we realized is that the rated capacitor value did not stay the same at 100 KHz on the impedance analyzer. The values consistently degraded by at least 30% of its rated capacitance. With this knowledge, we assumed the expected capacitance at 200 KHz would be even lower than that at 100 KHz. As suggested by Dr. Taufik, we performed tests on the capacitor and inductor to try and obtain more accurate values for the components.

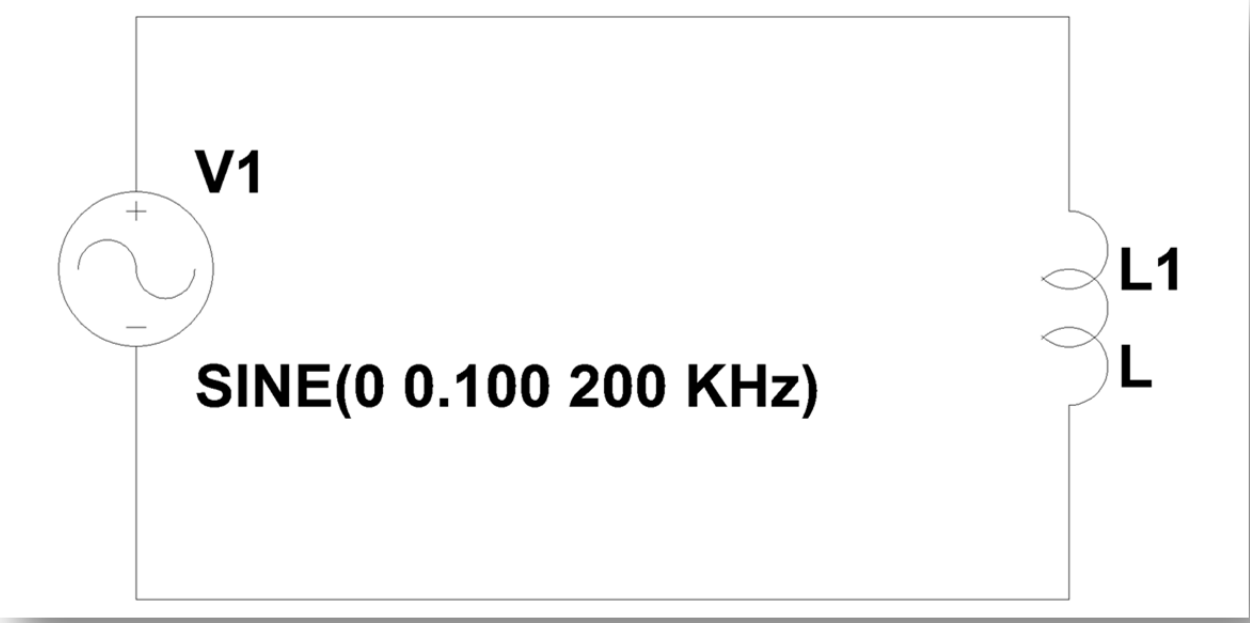

Figure 5-27: Circuit for calculation of inductance at 200 KHz

By setting up a 200 KHz signal with 0.1 V_{PP} (0.0707 V_{rms}), we would measure the RMS AC current through the inductor. We could then calculate explicitly for the reactance, and then the inductor value as shown below.

$$V = I * X_L \quad (5\text{-}3)$$

$$X_L = \frac{V}{I} \quad (5\text{-}4)$$

$$X_L = 2 * \Pi * f * L \quad (5\text{-}5)$$

$$\frac{V}{I} = 2 * \Pi * f * L \quad (5\text{-}6)$$

$$L = \frac{V}{2 * I * \Pi * f} \quad (5\text{-}7)$$

$$L = \frac{70mV_{RMS}}{2\Pi * (12mA_{RMS}) * (200{,}000\ Hz)} = 4.68\ \text{uH} \quad (5\text{-}8)$$

Knowing the actual inductance of our work coil with the core inside, we could now calculate the necessary capacitance needed for resonance at 200 KHz.

$$C = \frac{\left(\frac{1}{2 * \pi * f_O}\right)^2}{L} = \frac{\left(\frac{1}{2 * \pi * 200\ KHz}\right)^2}{4.68\ uH} = 135\ nF \quad (5\text{-}9)$$

With this knowledge, we could now test for individual capacitances to make a bank. We were able to find capacitors, through another test circuit, of 20 and 30 nF that are well suited for this purpose with their voltage ratings of 100V.

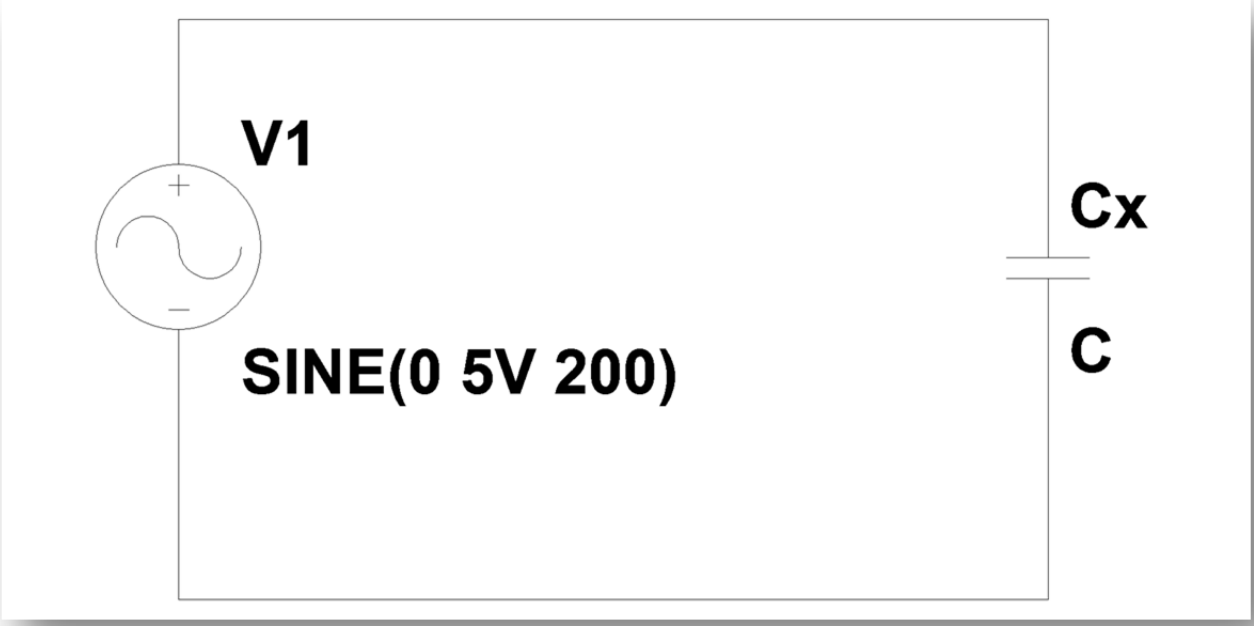

Figure 5-28: Circuit for calculation of capacitance at 200 KHz

The method for calculation of capacitances C_1 and C_2 is shown below.

$$V = I * X_C \quad (5\text{-}10)$$

$$X_C = \frac{V}{I} = \frac{1}{2*\pi*f*C} \quad (5\text{-}11)$$

$$\frac{1}{2*\pi*f*C} = \frac{V}{I} \quad (5\text{-}12)$$

$$\frac{I}{V*2*\pi*f} = C \quad (5\text{-}13)$$

$$C_1 = \frac{1.29mA}{3.5355V*2*\pi*200KHz} = 30nF \quad (5\text{-}14)$$

$$C_2 = \frac{89mA}{3.5355V*2*\pi*200KHz} = 20nF \quad (5\text{-}15)$$

These capacitors were assembled as shown in **Figure 5-29**.

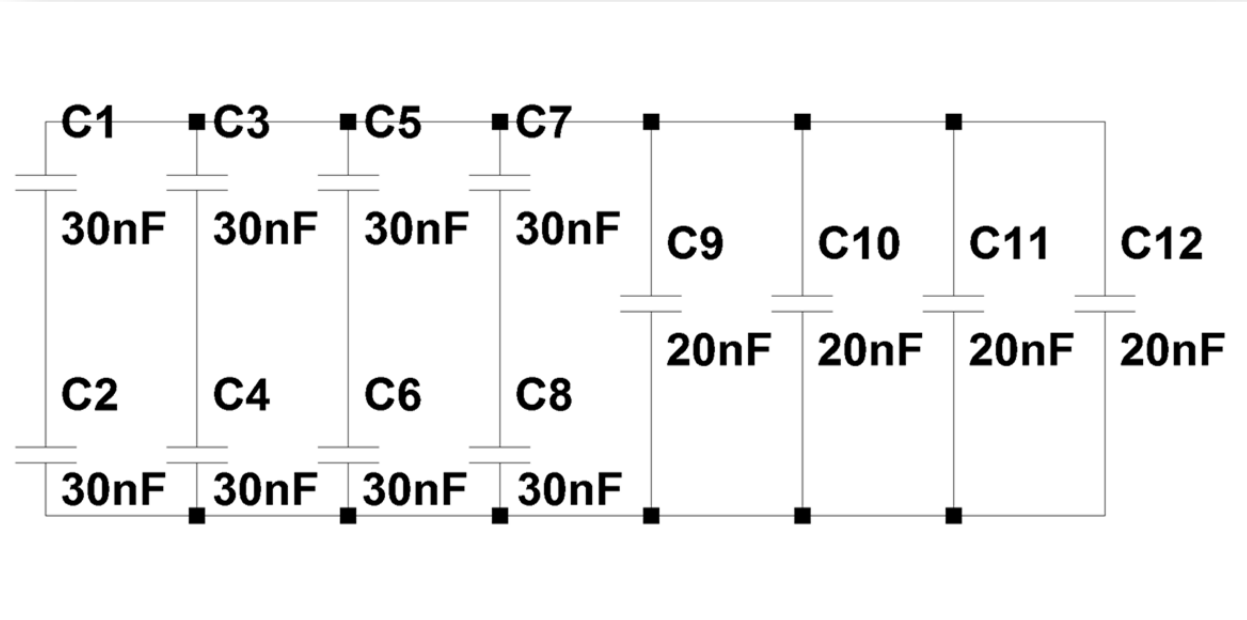

Figure 5-29: Capacitor bank configuration

This configuration of capacitors in series and in parallel gives us a bank with 140nF, which we believed was close enough to 135nF. We wanted to have a fair amount of branches for easier dissipation of heat amongst the capacitors. The ESR and the currents would quickly heat the capacitors. These branches help alleviate that strain on each capacitor. With this now set up, our work coil was ready to attach in parallel to the bank.

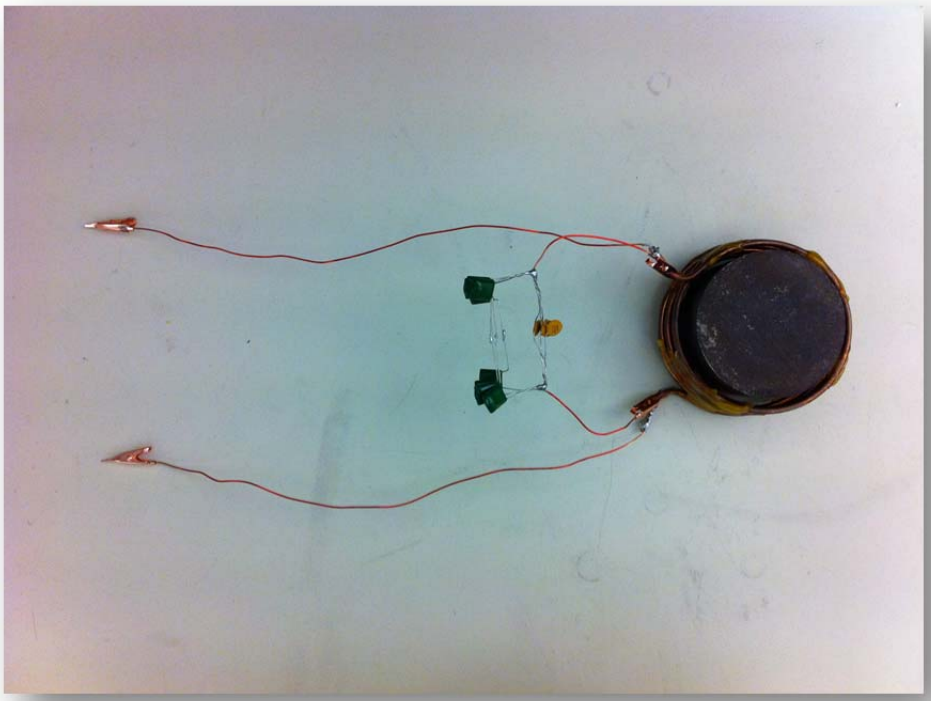

Figure 5-30: Our thin work coil in parallel with the capacitor bank

Load Four: Work coil with capacitive bank

The next step was to attach our LC-load to the H-bridge inverter. With the UBA2035 set to create a bridge frequency of 200 KHz and the LC-load designed to resonate at the mentioned frequency, we connected the load and powered the H-bridge as depicted in **Figure 5-31**.

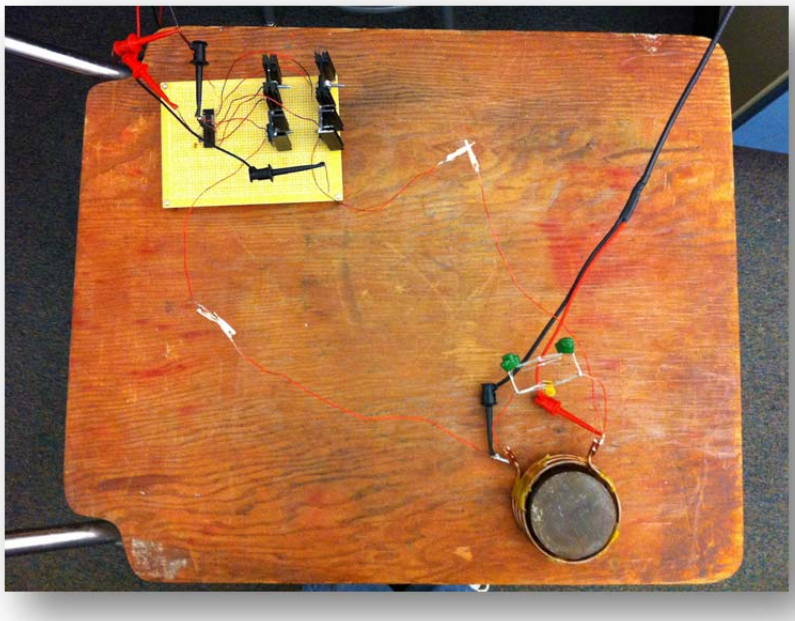

Figure 5-31: Fully loaded H-bridge inverter

Figure 5-32 displays the current through work coil at 192 KHz and using the equation 5-1, we can calculate the amplitude of the current to be as follows:

$$I_{per\ dision} = \frac{50mV/division}{10mV/division}\ x\ \left(\frac{1V}{division}\right) = 1\ A/division \qquad (5\text{-}16)$$

Using this information, and the figure above we calculated the current to be 4.25 $A_{PP.}$ This verifies the functionality of the H-bridge since we were sourcing a 4.35 A to the work coil.

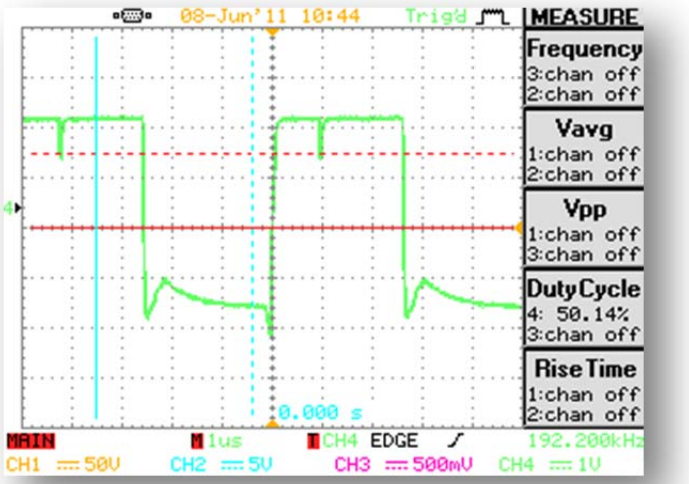

Figure 5-32: Current through work coil at 192 KHz

Using the 60V-30A DC power supply, we were able to drive 4.35A through the load at 192 KHz. Although not exactly at 200 KHz, this signal is still switching at a high frequency through the load, and still at 50% duty cycle.

The load voltage as shown in **Figure 5-33** is 3.41 and not the value of V_{DD}. The reason for this is we limited the current flowing through the MOSFETS due to low current rating [5]. The highest current rating that the MOSFET can withstand is 6A, and it was already at 4.35A. We chose to limit the current to this level because this is the expected output current from the solar panels in our design.

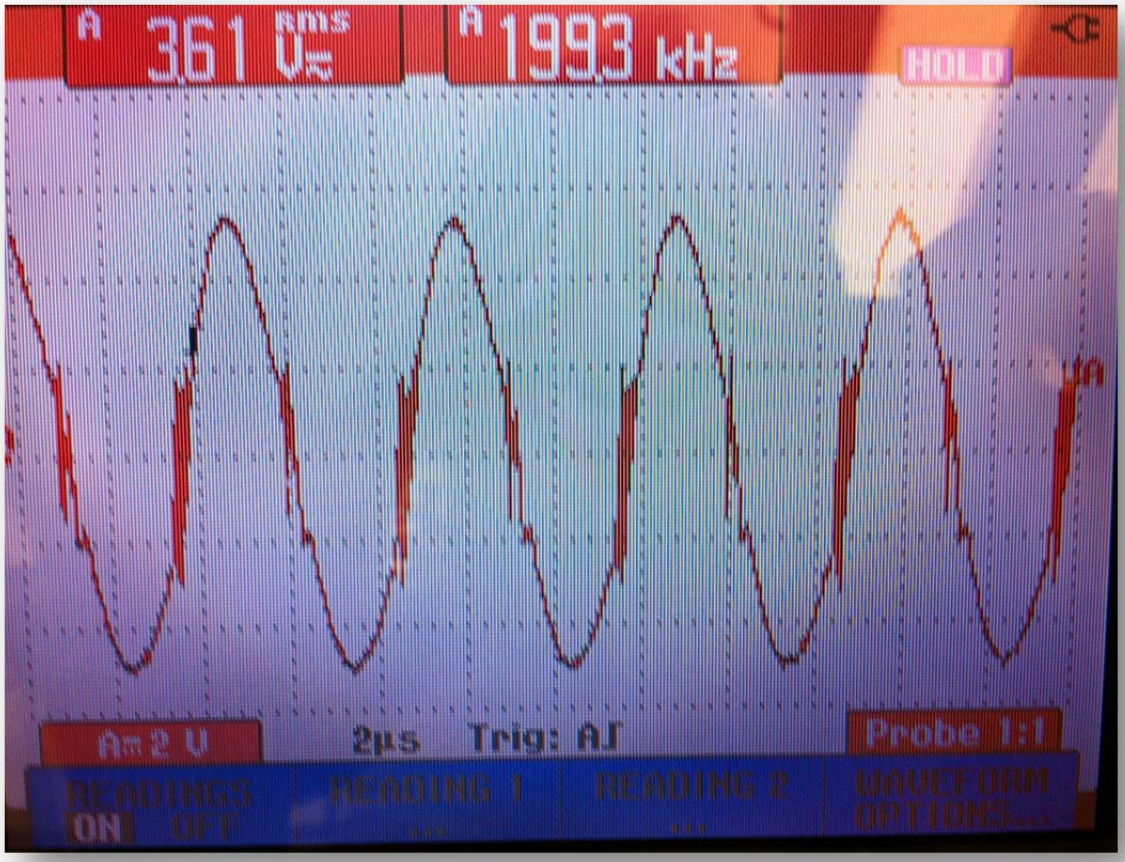

Figure 5-33: Voltage seen across load

Condensation System

Some ideas were considered for this system. The first one was to build a stand made of PVC piping. The problem with this approach is that when the stand gets warm, the piping will bend and warp. AVS piping is expensive, and harder to assemble a freestanding system. Another approach was to use wood as our frame. Wood is strong, cheap, and easy to manipulate and assemble. For our prototype of this system, we determined that a wood frame would be the least expensive to build and easiest to replicate (for others). We decided a 5' stand would give us enough clearance for the rest of the components for the system and would also allow us to install a foldable mount for holding up our circuit and work coil. To secure the wooden pole, four 16" wooden feet were added. Since portability is one of our main concerns, wheels were attached underneath the feet. Altogether, the standing wooden mechanism has a weight of approximately 13 pounds as shown in **Figure 5-34**.

Figure 5–34: Standing wooden pole with feet

Once the standing post was assembled and ready, the next step was to mount the selected components. As seen in **Figure 5-35** the first element we glued together was the heat exchanger. To glue these elements together, ABS cement was used since this glue can withstand high temperatures and still hold.

Figure 5-35: Disassembled heat exchange chamber

The internal piping that runs through the heat exchanger can be seen in **Figure 5-36**. The cold water that sits outside the thin pipe will help condensate the hot steam flowing the thin pipe inside the heat exchanger.

Figure 5-36 Inside-view of cooling chamber

As seen in **Figure 5-37**, the funnel is used to pour cold water into the chamber. The white PVC pipe is used to guide the steam through the inside, alongside the cold water.

Figure 5-37: Side view of completed heat exchanger.

From the end of the heat exchanger, the PVC piping leads into one last element as shown in **Figure 5-38**. This is the clean water container. This 1-gallon ABS pipe allows for further condensation of the steam with its internal space. This gives the steam one last phase to condense into water. By giving the steam more space to spread out on to the walls the volume of water that will condense will increase compared to the PVC pipe in the system.

Figure 5 -38: Integration of heat exchanger and water container.

After final checks were done, no water leakages were present. The next step was to build a connector that will could fit our into the aluminum pot shown in **Figure 5-39.** The aluminum pot is basically a drink mixer that we thought could satisfy our necessities in terms of selecting a container with thin walls and itself being good heat container. For testing purposes we bought a slow cooker as a way of using it as a hot plate to heat up the water container and boil water for testing. Several tests were done using this method: the first one using the drink mixer and the other using the slow cooker as the container to boil the water. It turns out that using the slow cooker gives us a more efficient way to purify water since we get more steam flowing thru the PVC pipes, which means more pressure.

Figure 5-39: Full water-purifying system

With enough pressure to propel the steam through the pipes, the condensation system was able to successfully boil and condensate water. Right now, the current system is not very efficient. At present, it takes 20 minutes to begin to boil 72 ounces of water when the boiler is set to 400 degrees. After this first period, it takes another 15 minutes to condensate only 12 ounces of water. This gives it an efficiency of 16% based on water input vs. water output.

CONCLUSION

Our objective for this project was a proof of concept: that we could make a portable solar desalinization unit using solar panels, an H-bridge inverter, a work coil with a core inside, and vapor distillation. Creating a system that uses solar power to clean water is not a very simple task by any means. Size and cost of components were a big issue with our design because we want it to be portable and cheap at the same time. Studying and learning different design topologies was very time consuming and left us feeling like we hit a dead end when we found one idea wouldn't work. Through the course of this project we learned a great deal about converting DC to AC. Through the use of the UBA2035 full bridge driver, the conversion from DC to AC at a reasonably cheap value is possible. The use of an inductor coil to generate heat with flux makes gives us the energy we need for vapor distillation. We didn't know about inductive heating before this project, and now we are using that technology to distill water. Although this project has come to an end, improvements could still be made.

We were able to make the H-bridge inverter that could work with the BPX150S solar panel and would sink 4.35A. This H-bridge prototype would not be able to stay on for very long due to the MOSFETs heating up very quickly. A method of cooling the MOSFETs more rapidly would allow the H-bridge inverter to be tested further. The controller we were using was unable to drive the power MOSFETs we had selected for sinking 8A. This prevented the H-bridge inverter from being attached to the solar panels for testing. We believe that the UBA2035 chip is simply not compatible with the IXFH40N30 power MOSFETs. These being high-powered switches, we believe that the controller cannot drive the gates with enough power.

The work coils were made out of copper, and wound properly with even gap spacing. But with the H-bridge prototype we constructed not sinking the current we wanted to, we never did find out if the core we had would actually produce enough heat for boiling. The unexpected length of time for the H-bridge construction contributed to not having further testing with the work coil and core. Further research needs to be done which relates the amount of flux produced by the high frequency AC current will generate a certain amount of heat. Another topic to be explored would be Dr. Dolan's advice concerning the work core: to determine the best frequency to maximize heat generation through core losses. That process alone is enough work for one senior project itself.

The condensation system did work. It used heat to boil water into steam, and condense it back into water. A few improvements on the system could increase the efficiency. Sixteen percent is too low. New ideas could be approached on how to cool the steam down fast enough, which would maximize the water used. One idea we believe would condense the steam faster is if we ran multiple tubes down through the heat exchanger. More steam would then be able to condense. The piping would also need to be replaced with non-plastic materials, such as copper tubing. When hot steam is run through PVC piping, there is a chance that chemicals not safe for drinking will be released by the steams heat and absorbed in the water. Copper tubing would not suffer this problem.

We feel good knowing that our project can grow into something very useful for people who struggle to get clean drinking water. This project allowed us to use engineering in the very fundamental sense of the word: using science, mathematics, and sources of energy to be made into something useful for the benefit of humanity.

The unexpected length of time used to properly build the inverter prevented us from having enough time to properly test powering the H-bridge inverter with the solar panels. Without this connection, we were not able to fully construct the system we designed.

BIBLIOGRAPHY

[1] "Clean Water For The World." *Clean Water For The World*. Web. 01 Apr. 2011. <http://www.cleanwaterfortheworld.org/>.

[2] “Smart Power and Water for Challenging Environments” Web 01 Apr. 2011. <http://robots.mit.edu/projects/KFUPM/index.html>

[3] “Ameritherm Co” Web 08 Apr. 2011. <http://www.amertherm.com>

[4] UBA2035 datasheet, Rev. 01-31 October 2008

[5] STP6NK60Z datasheet, May 2002

[6] Dr. Taufik’s lecture notes of EE 410 and EE 433

Appendices

PART LIST AND COST

H-Bridge

Qty	Component	Cost per unit ($)
1	UBA2035 full bridge driver IC	1.83
8	30nF,100V capacitor	0.17
4	20nF,100V capacitor	0.15
1	1nF capacitor	1.15
1	Protoboard	2.19
1	100KΩ resistor	0.84
1	CopperBond Epoxy	5.45
1	Set of 22 gauge wires	5.35
1	Package of grabbers	2.50
4	STP6NK60Z MOSFETS	1.69
1	BP SX 150S Solar Panel	0

Total H-Bridge Cost	22.96

Work Coil

Qty	Component	Cost per unit ($)
1	10-guage copper wire	3.45
1	13-gauge copper wire	3.45

Total Work Coil Cost	6.90

Condensation System

Qty	Component	Cost per unit ($)
4	¾ " PVC Elbows	2.28
1	5' PVC piping	4.27
1	Funnel	1.47
1	ABS black tube	10.95
4	ABS Caps	33.27
1	ABS Cement	4.19
2	No-kink valves	18.68
1	Wood Screws	2.00
2	Bronze Hinges	2.78
4	Corner Braces	7.94
1	Package, 4 wheels	4.96
1	Wood	0

Total Condensation System Cost	120.51